Ministry for Primary Industries
Manatū Ahu Matua

The 2011 stock assessment of paua (*Haliotis iris*) for PAU 7

New Zealand Fisheries Assessment Report 2012/27

D. Fu

ISSN 1179-5352 (online)
ISBN 978-0-478-38889-3 (online)

June 2012

New Zealand Government

Growing and Protecting New Zealand

Requests for further copies should be directed to:

Publications Logistics Officer
Ministry for Primary Industries
PO Box 2526
WELLINGTON 6140

Email: brand@mpi.govt.nz
Telephone: 0800 00 83 33
Facsimile: 04-894 0300

This publication is also available on the Ministry for Primary Industries websites at:
http://www.mpi.govt.nz/news-resources/publications.aspx
http://fs.fish.govt.nz go to Document library/Research reports

Table of Contents

EXECUTIVE SUMMARY

Fu, D. (2012). The 2011 stock assessment of paua (*Haliotis iris*) for PAU 7

***New Zealand Fisheries Assessment Report 2012/27*. 56 p.**

This report summarises the stock assessment for PAU 7 with the inclusion of fishery data up to the 2010–11 fishing year. The report describes the model structure and output, including current and projected stock status. The stock assessment is implemented as a length-based Bayesian estimation model, with point estimates of parameters based on the mode of the joint posterior distribution, and uncertainty of model estimates investigated using the marginal posterior distributions generated from Markov chain-Monte Carlo simulation.

The data fitted in the assessment model were: (1) a standardised CPUE series based on the early CELR data, (2) a standardised CPUE series based on recent PCELR data, (3) a standardised research diver survey index (RDSI), (4) a research diver survey length frequency series (RDLF), (5) a commercial catch sampling length frequency series (CSLF), (6) tag-recapture length increment data, and (7) maturity-at-length data.

Iterative re-weighting of the datasets produced an initial model in which the standard deviations of the normalised residuals were close to unity for most datasets. For the base case, the RDLF and CSLF data were down-weighted using an alternative weighting method which accounted for correlations in the proportion-at-length data. However, estimates of biomass indicators and stock status were similar between the initial model and the base case.

The base case model appears to have represented most observational data well, and there is no obvious indication of lack of fit. The CPUE shape parameter was estimated to be less than 1, suggesting a possible hyper-stability relationship between CPUE and abundance. Model results changed very little when a linear relationship between CPUE and abundance was assumed. Sensitivity runs assuming a different stock-recruitment steepness parameter or maximum exploitation rate showed similar model fits and estimates of abundance.

The base case estimated growth parameters within the model and incorporated the tag-recapture data. The fits to the tag-recapture data appear adequate, but are likely to have been influenced by the proportion-at-length data. Sensitivity runs assuming alternative growth parameters (fixed at values representing either a fast or slow growth rate) led to significant changes to the estimates of abundance, but had poor fits to the proportion-at-length data.

Current estimates from the base case suggested that the current spawning stock population was about 22% (19–26%) of the virgin level, and the recruit-sized stock abundance was about 10% (8–12%) of the initial state. The model projection, made for three years assuming current catch levels and using recruitments re-sampled from the recent model estimates suggested that the spawning stock abundance will increase slightly to about 23.4% (17–32%) B_0 over the next three years. Projections made with alternative catch levels showed that the spawning stock abundance will increase to about 24.4%, 25.0%, and 25.5% of B_0, if the commercial catch was reduced by 10%, 15%, and 20% respectively.

The potential impact of introducing areas closed to commercial fishing in PAU 7 was assessed via projections made with the assumption that the loss of productivity in the closed area was proportional to its historical catch. The projections were made for scenarios where Tory channel, D'Urville, and the West coast are alienated accumulatively and their catches are displaced. The results suggested that the future stock abundance is likely to decline under these scenarios, but the risk of this occurring is significantly reduced if the future commercial catch is reduced by up to 20%.

1. INTRODUCTION

1.1 Overview

This report summarises the stock assessment for PAU 7 (at the northern end of the South Island, Figure 1) with the inclusion of data to the end of 2010–11 fishing year. The report describes the model structure and output, including current and projected stock status. The stock assessment is conducted with the length-based Bayesian estimation model first used in 1999 for PAU 5B (Breen et al. 2000a) and revised for subsequent assessments in PAU 5B (Breen et al. 2000b) and PAU 7 (Andrew et al. 2000, Breen & Kim 2003, 2005, McKenzie & Smith 2009) with revisions made for PAU 4 (Breen & Kim 2004a) and PAU 5A (Breen & Kim 2004b) in 2004 mostly discarded. The model was published by Breen et al. (2003).

Most catches have been taken from Statistical Areas 017 and 038. There is no time series of research diver surveys from outside these areas (Figure 2). Accordingly, Breen et al. (2001) and Breen & Kim (2003, 2005), and McKenzie & Smith (2009) based their assessments on Statistical Areas 017 and 038 only. The Shellfish Fishery Assessment Working Group agreed to continue this practice for this assessment.

The seven sets of data fitted in the assessment model were: (1) a standardised CPUE series covering 1990–2001 based on CELR data (CPUE), (2) a standardised CPUE series covering 2002–2010 based on PCELR data (PCPUE), (3) a standardised research diver survey index (RDSI), (4) a research diver survey proportions-at-lengths series (RDLF), (5) A commercial catch sampling length frequency series (CSLF), (6) tag-recapture length increment data, and (7) maturity-at-length data. Catch history was an input to the model, encompassing commercial, recreational, customary, and illegal catch. Another document describes the datasets that are used in the stock assessment and the updates that were made for the previous assessment (Fu et al. 2012).

The assessment was made in several steps. First, the model was fitted to the data with arbitrary weights on the various datasets. The weights were then iteratively adjusted to produce balanced residuals among the datasets where the standard deviation of the normalised residuals was close to one for each dataset. The fit obtained is the mode of the joint posterior distribution of parameters (MPD). Next, from the resulting fit, Markov chain-Monte Carlo (MCMC) simulations were made to obtain a large set of samples from the joint posterior distribution. From this set of samples, forward projections were made with a set of agreed indicators obtained. Sensitivity trials were explored by comparing MPD fits made with alternative model assumptions. The model was then used to make projections under scenarios where areas are alienated and catch is displaced, to assess the potential impact of introducing areas closed to commercial fishing.

This document describes the model structure and assumptions, the fits to the data, estimates of parameters and indicators, and projection results. This report fulfils Objective 1 "Undertake a stock assessment for PAU 7, using a length-based Bayesian model", and Objective 2 "Assess the effects of a decrease in areas available to commercial fishing on the sustainability of the fishery under the current TACC" of Project PAU2011/06.

1.2 Description of the fishery

The paua fishery was summarised by Schiel (1992), and in numerous previous assessment documents (e.g., Schiel 1989, McShane et al. 1994, 1996, Breen et al. 2000a, 2000b, 2001, Breen & Kim 2003, 2004a, 2004b, 2007). A further summary is not presented here.

2. MODEL

This section gives an overview of the model used for stock assessment of PAU 7 in 2011; for full description see Breen et al. (2003). The model was developed for use in PAU 5B in 1999 and has been revised each year for subsequent assessments, in many cases echoing changes made to the rock lobster assessment model (Kim et al. 2004), which is a similar but more complex length-based Bayesian model. Only minor changes were made to the last revision which was the 2008 assessment model of PAU 7 (McKenzie & Smith 2009), the main change being that a penalty function was imposed to encourage the mean of recruitment deviation to be close to one.

2.1 Model description

The model partitioned the paua stock into a single sex population, with length classes from 70 mm to 170 mm, in groups of 2 mm (i.e., from 70 to under 72 mm, 72 mm to under 74 mm, etc.). The largest length bin is well above the maximum size observed. The stock was assumed to reside in a single, homogeneous area. The partition accounted for numbers of paua by length class within an annual cycle, where movement between length classes was determined by the growth parameters. Paua entered the partition following recruitment and were removed by natural mortality and fishing mortality.

The model annual cycle was based on the fishing year. Note that model references to "year" within this paper refer to the fishing year, and are labelled as the most recent calendar year, i.e., the fishing year 1998–99 is referred to as "1999" throughout. References to calendar years are denoted specifically.

The models were run for the years 1965–2011. Catches were collated for 1974–2011, and were assumed to increase linearly between 1965 and 1973 from 0 to the 1974 catch level. Catches included commercial, recreational, customary, and illegal catch, and all catches occurred at the same time step.

Recruitment was assumed to take place at the beginning of the annual cycle, and length at recruitment was defined by a uniform distribution with a range between 70 and 80 mm. Recruitment deviations were assumed known and equal to 1 for the years up to 1980. This was ten years before the length data were available (loosely based on the approximate time taken for recruited paua to appear at the right hand end of the length distribution). The stock-recruitment relationship is unknown for paua, but is likely to be weak (Shepherd et al. 2001). A relationship may exist on small scales, but may not be apparent when large-scale data are modelled (Breen et al. 2003). No explicit stock-recruitment relationship has been modelled in previous assessments. The Shellfish Working Group suggested assuming a Beverton-Holt stock-recruitment relationship with a steepness of 0.75 for the base case.

Maturity does not feature in the population partition. The model estimated proportions mature with the inclusion of length-at-maturity data. Growth and natural mortalities were also estimated within the model.

The models used two selectivities: the commercial fishing selectivity and research diver survey selectivity — both assumed to follow a logistic curve (see later) and then remain constant.

The model is implemented in AD Model Builder™ (Otter Research Ltd., http://otter-rsch.com/admodel.htm) version 9.0.65, compiled with the MinGW 4.50 compiler.

2.1.1 Estimated parameters

Parameters estimated by the model are as follows. The parameter vector is referred to collectively as θ.

$\ln(R0)$	natural logarithm of base recruitment
M	instantaneous rate of natural mortality
g_1	expected annual growth increment at length L_1
g_2	expected annual growth increment at length L_2
ϕ	c.v. of the expected growth increment
α	parameter that defines the variance as a function of growth increment
β	parameter that defines the variance as a function of growth increment
$\Delta_{\max}$	maximum growth increment
l_{50}^{g}	length at which the annual increment is half the maximum
l_{95}^{g}	length at which the annual increment is 95% of the maximum
l_{95-50}^{g}	difference between l_{50}^{g} and l_{95}^{g}
q^{I}	scalar between recruited biomass and CPUE
q^{I_2}	scalar between recruited biomass and PCPUE
q^{J}	scalar between numbers and the RDSI
L_{50}	length at which maturity is 50%
L_{95-50}	interval between L_{50} and L_{95}
T_{50}	length at which research diver selectivity is 50%
T_{95-50}	difference between T_{50} and T_{95}
D_{50}	length at which commercial diver selectivity is 50%
D_{95-50}	difference between D_{50} and D_{95}
$\widetilde{\sigma}$	common component of error
h	shape of CPUE *vs.* biomass relation
ε	vector of annual recruitment deviations, estimated from 1977 to 2004
H	steepness of the Beverton-Holt stock-recruitment relationship

2.1.2 Constants

l_k	length of a paua at the midpoint of the k^{th} length class (l_k for class 1 is 71 mm, for class 2 is 73 mm and so on)
σ_{MIN}	minimum standard deviation of the expected growth increment (assumed to be 1 mm)
σ_{obs}	standard deviation of the observation error around the growth increment (assumed to be 0.25 mm)
MLS_t	minimum legal size in year t (assumed to be 125 mm for all years)
$P_{k,t}$	a switch based on whether abalone in the k^{th} length class in year t are above the minimum legal size (MLS) ($P_{k,t} = 1$) or below ($P_{k,t} = 0$)
a, b	constants for the length-weight relation, taken from Schiel & Breen (1991) (2.592E-08 and 3.322 respectively, giving weight in kg)

w_k	the weight of an abalone at length l_k
ϖ^I	relative weight assigned to the CPUE dataset. This and the following relative weights were varied between runs to find a basecase with balanced residuals
ϖ^{I2}	relative weight assigned to the PCPUE dataset.
ϖ^J	relative weight assigned to the RDSI dataset
ϖ^r	relative weight assigned to RDLF dataset
ϖ^s	relative weight assigned to CSLF dataset
ϖ^{mat}	relative weight assigned to maturity-at-length data
ϖ^{tag}	relative weight assigned to tag-recapture data
κ_t^s	normalised square root of the number of paua measured greater than 113 mm in CSLF records for each year, normalised by the lowest year
κ_t^r	normalised square root of the number of paua measured greater than 89 mm in RDLF records for each year, normalised by the lowest year
$U^{\max}$	exploitation rate above which a limiting function was invoked (0.80 for the base case)
μ_M	mean of the prior distribution for *M*, based on a literature review by Shepherd & Breen (1992)
σ_M	assumed standard deviation of the prior distribution for *M*
σ_ε	assumed standard deviation of recruitment deviations in log space (part of the prior for recruitment deviations)
n_ε	number of recruitment deviations
L_1	length associated with g_1 (75 mm)
L_2	length associated with g_2 (120 mm)

2.1.3 Observations

C_t	observed catch in year *t*
I_t	standardised CPUE in year *t*
$I2_t$	standardised PCPUE in year *t*
σ_t^I	standard deviation of the estimate of observed CPUE in year *t*, obtained from the standardisation model
σ_t^{I2}	standard deviation of the estimate of observed PCPUE in year *t*, obtained from the standardisation model
J_t	standardised RDSI in year *t*
σ_t^J	the standard deviation of the estimate of RDSI in year t, obtained from the standardisation model
$p_{k,t}^r$	observed proportion in the k^{th} length class in year *t* in RDLF
$p_{k,t}^s$	observed proportion in the k^{th} length class in year *t* in CSLF
l_j	initial length for the j^{th} tag-recapture record
d_j	observed length increment of the *j*th tag-recapture record
Δt_j	time at liberty for the j^{th} tag-recapture record

p_k^{mat}	observed proportion mature in the k^{th} length class in the maturity dataset

2.1.4 Derived variables

$R0$	base number of annual recruits
$N_{k,t}$	number of paua in the k^{th} length class at the start of year t
$N_{k,t+0.5}$	number of paua in the k^{th} length class in the mid-season of year t
$R_{k,t}$	recruits to the model in the k^{th} length class in year t
g_k	expected annual growth increment for paua in the k^{th} length class
σ^{g_k}	standard deviation of the expected growth increment for paua in the k^{th} length class, used in calculating $\mathbf{G}$
$\mathbf{G}$	growth transition matrix
B_t	spawning stock biomass at the beginning of year t
$B_{t+0.5}$	spawning stock biomass in the mid-season of year t
B_0	equilibrium spawning stock biomass assuming no fishing and average recruitment from the period in which recruitment deviations were estimated.
B_{init}	spawning stock biomass at the end of initialisation phase (or B_{1964})
B_t^r	biomass of paua above the MLS at the beginning of year t
$B_{t+0.5}^r$	biomass of paua above the MLS in the mid-season of year t
B_0^r	equilibrium biomass of paua above the MLS assuming no fishing and average recruitment from the period in which recruitment deviations were estimated
B_{init}^r	biomass of paua above the MLS at the end of initialisation phase (or B_{1964}^r)
U_t	exploitation rate in year t
A_t	the complement of exploitation rate
$SF_{k,t}$	finite rate of survival from fishing for paua in the kth length class in year t
V_k^r	relative selectivity of research divers for paua in the kth length class
V_k^s	relative selectivity of commercial divers for paua in the kth length class
$\sigma_{k,t}^r$	error of the predicted proportion in the k^{th} length class in year t in RDLF data
n_t^r	relative weight (effective sample size) of the RDLF data in year t
$\sigma_{k,t}^s$	error of the predicted proportion in the k^{th} length class in year t in CSLF data
n_t^s	relative weight (effective sample size)of the CSLF data in year t
σ_j^d	standard deviation of the predicted length increment for the j^{th} tag-recapture record
σ_j^{tag}	total error predicted for the j^{th} tag-recapture record
σ_k^{mat}	error of the proportion mature-at-length for the k^{th} length class
$-\ln(\mathbf{L})$	negative log-likelihood
f	total function value

2.1.5 Predictions

$\hat{I}_t$	predicted CPUE in year *t*
$\hat{I}2_t$	predicted PCPUE in year *t*
$\hat{J}_t$	predicted RDSI in year *t*
$\hat{p}^r_{k,t}$	predicted proportion in the k^{th} length class in year *t* in research diver surveys
$\hat{p}^s_{k,t}$	predicted proportion in the k^{th} length class in year *t* in commercial catch sampling
$\hat{d}_j$	predicted length increment of the j^{th} tag-recapture record
$\hat{p}^{mat}_k$	predicted proportion mature in the k^{th} length class

2.1.6 Initial conditions

The initial population is assumed to be in equilibrium with zero fishing mortality and the base recruitment. The model is run for 60 years with no fishing to obtain near-equilibrium in numbers-at-length. Recruitment is evenly divided among the first five length bins:

(1) $R_{k,t} = 0.2R0$ for $1 \le k \le 5$

(2) $R_{k,t} = 0$ for $k > 5$

A growth transition matrix is calculated inside the model from the estimated growth parameters. If the growth model is linear, the expected annual growth increment for the *k*th length class is:

(3) $$\Delta l_k = \left(\frac{L_2 g_1 - L_1 g_2}{g_1 - g_2} - l_k \right) \left[1 - \left(1 + \frac{g_1 - g_2}{L_1 - L_2} \right) \right]$$

The model uses the AD Model Builder™ function *posfun*, with a dummy penalty, to ensure a positive expected increment at all lengths, using a smooth differentiable function. The *posfun* function is also used with a real penalty to force the quantity $\left(1 + \frac{g_1 - g_2}{L_1 - L_2} \right)$ to remain positive. If the growth model is exponential (used for the base case), the expected annual growth increment for the *k*th length class is:

(4) $$\Delta l_k = g_1 \left(g_2 / g_1 \right)^{(l_k - L_1)/(L_2 - L_1)}$$

again using posfun with a dummy penalty to ensure a positive expected increment at all lengths. If the inverse logistic growth model is used), the expected annual growth increment for the *k*th length class is:

(5) $$\Delta l_k = \frac{\Delta_{\max}}{\left(1 + \exp\left(\ln(19) \left(\left(l_k - l^g_{50} \right) / \left(l^g_{95} - l^g_{50} \right) \right) \right) \right)}$$

The standard deviation of g_k is assumed to be proportional to g_k with minimum σ_{MIN}:

$$\sigma^{g_k} = \left(g_k\phi - \sigma_{MIN}\right)\left(\frac{1}{\pi}\tan^{-1}\left(10^6\left(g_k\phi - \sigma_{MIN}\right)\right) + 0.5\right) + \sigma_{MIN} \quad (6)$$

Or a more complex functional form between the growth increment and its standard deviation can be defined as:

$$\sigma^{g_k} = \left(\alpha\left(g_k\right)^{\beta} - \sigma_{MIN}\right)\left(\frac{1}{\pi}\tan^{-1}\left(10^6\left(\alpha\left(g_k\right)^{\beta} - \sigma_{MIN}\right)\right) + 0.5\right) + \sigma_{MIN} \quad (7)$$

From the expected increment and standard deviation for each length class, the probability distribution of growth increments for a paua of length l_k is calculated from the normal distribution and translated into the vector of probabilities of transition from the k^{th} length bin to other length bins to form the growth transition matrix **G**. Zero and negative growth increments are permitted, i.e., the probability of staying in the same bin or moving to a smaller bin can be non-zero.

In the initialisation, the vector $\mathbf{N_t}$ of numbers-at-length is determined from numbers in the previous year, survival from natural mortality, the growth transition matrix **G,** and the vector of recruitment $\mathbf{R_t}$:

$$\mathbf{N_t} = \left(\mathbf{N_{t\text{-}1}}\, e^{-M}\right) \bullet \mathbf{G} + \mathbf{R_t} \quad (8)$$

where the dot (•) denotes matrix multiplication.

2.1.7 Dynamics

2.1.7.1 Sequence of operations

After initialising, the first model year is 1965 and the model is run through to 2009. In the first nine years the model is run with an assumed catch vector, because it is unrealistic to assume that the fishery was in a virgin state when the first catch data became available in 1974. The assumed catch vector rises linearly from zero to the 1974 catch. These years can be thought of as an additional part of the initialisation, but they use the dynamics described in this section.

Model dynamics are sequenced as follows.

- Numbers at the beginning of year *t*-1 are subjected to fishing, then natural mortality, then growth to produce the numbers at the beginning of year *t*.
- Recruitment is added to the numbers at the beginning of year *t*.
- Biomass available to the fishery is calculated and, with catch, is used to calculate the exploitation rate, which is constrained if necessary.
- Half the exploitation rate (but no natural mortality) is applied to obtain mid-season numbers, from which the predicted abundance indices and proportions-at-length are calculated. Mid-season numbers are not used further.

2.1.7.2 Main dynamics

For each year *t*, the model calculates the start-of-the-year biomass available to the commercial fishery. Biomass available to the commercial fishery is:

$$B_t = \sum_k N_{k,t} V_k^s w_k \quad (9)$$

$$V_k^{t,s} = \frac{1}{1+19^{-\left((l_k - D_{50})/D_{95-50}\right)}} \quad \text{for } t < 2007 \quad (10)$$

$$V_k^{t,s} = \frac{1}{1+19^{-\left((l_k - D_{50} - 5)/D_{95-50}\right)}} \quad \text{for } t \geq 2007 \quad (11)$$

The observed catch is then used to calculate the exploitation rate, constrained for all values above U^{max} with the *posfun* function of AD Model Builder™. If the ratio of catch to available biomass exceeds U^{max}, then exploitation rate is constrained and a penalty is added to the total negative log-likelihood function. Let minimum survival rate A_{min} be 1-U^{max} and survival rate A_t be 1-U_t:

$$A_t = 1 - \frac{C_t}{B_t} \quad \text{for } \frac{C_t}{B_t} \leq U^{\max} \quad (12)$$

$$A_t = 0.5 A_{\min}\left[1 + \left(3 - \frac{2\left(1 - \frac{C_t}{B_t}\right)}{A_{\min}}\right)^{-1}\right] \quad \text{for } \frac{C_t}{B_t} > U^{\max} \quad (13)$$

The penalty invoked when the exploitation rate exceeds U^{max} is:

$$1000000\left(A_{\min} - \left(1 - \frac{C_t}{B_t}\right)\right)^2 \quad (14)$$

This prevents the model from exploring parameter combinations that give unrealistically high exploitation rates. Survival from fishing is calculated as:

$$SF_{k,t} = 1 - (1 - A_t) P_{k,t} \quad (15)$$

or

$$SF_{k,t} = 1 - (1 - A_t) V_k^s \quad (16)$$

The vector of numbers-at-length in year *t* is calculated from numbers in the previous year:

$$\mathbf{N_t} = \left(\left(\mathbf{SF_{t-1}} \otimes \mathbf{N_{t-1}}\right) e^{-M}\right) \bullet \mathbf{G} + \mathbf{R_t} \quad (17)$$

where $\otimes$ denotes the element-by-element vector product. The vector of recruitment, $\mathbf{R_t}$, is determined from *R0*, estimated recruitment deviations, and the stock-recruitment relationship:

(18) $$R_{k,t} = 0.2R0e^{\left(\varepsilon_t - 0.5\sigma_t^2\right)} \frac{B_{t-1+0.5}}{B_0} \Big/ \left(1 - \frac{5H-1}{4H}\left(1 - \frac{B_{t-1+0.5}}{B_0}\right)\right) \qquad \text{for } 1 \le k \le 5$$

(19) $$R_{k,t} = 0 \qquad \text{for } k > 5$$

The recruitment deviation parameters ε_t were estimated for all years from 1980. The recruitment deviations were constrained to have a mean of 1 in arithmetic space.

The model predicts CPUE in year *t* from mid-season recruited biomass, the scaling coefficient, and the shape parameter:

(20) $$\hat{I}_t = q^I \left(B_{t+0.5}\right)^h$$

Available biomass $B_{t+0.5}$ is the mid-season vulnerable biomass after half the catch has been removed (no natural mortality is applied, because the time over which half the catch is removed might be short). It is calculated as in equation (9), but using the mid-year numbers, $N_{k,t+0.5}$:

(21) $$N^{vuln}_{k,t+0.5} = N_{k,t}\left(1 - \frac{\left(1-A_t\right)}{2} V^s_k\right).$$

Similarly,

(22) $$\hat{I}2_t = q^{I2}\left(B_{t+0.5}\right)^h = Xq^I\left(B_{t+0.5}\right)^h$$

The same shape parameter *h* is used for both series: experimentation outside the model showed that this was appropriate despite the different units of measurement for the two series. The predicted research diver survey index is calculated from mid-season model numbers in bins greater than 89 mm length, taking into account research diver selectivity-at-length:

(23) $$N^{res}_{k,t+0.5} = N_{k,t}\left(1 - \frac{\left(1-A_t\right)}{2} V^r_k\right)$$

(24) $$\hat{J}_t = q^J \sum_{k=11}^{55} N^{res}_{k,t+0.5}$$

where the scalar is estimated and the research diver selectivity V^r_k is calculated from:

(25) $$V^r_k = \frac{1}{1+19^{-\left(\left(l_k - T_{50}\right)/T_{95-50}\right)}}$$

The model predicts proportions-at-length for the RDLF from numbers in each length class for lengths greater than 89 mm:

(26) $$\hat{p}^{r}_{k,t} = \frac{N^{res}_{k,t+0.5}}{\sum_{k=11}^{51} N^{res}_{k,t+0.5}} \qquad \text{for } 11 \le k < 51$$

Predicted proportions-at-length for CSLF are similar:

(27) $$\hat{p}^{s}_{k,t} = \frac{N^{vuln}_{k,t+0.5}}{\sum_{k=23}^{51} N^{vuln}_{k,t+0.5}} \qquad \text{for } 23 \le k < 51$$

The predicted increment for the *j*th tag-recapture record, using the linear model, is:

(28) $$\hat{d}_j = \left(\frac{\beta g_\alpha - \alpha g_\beta}{g_\alpha - g_\beta} - L_j \right) \left[1 - \left(1 + \frac{g_\alpha - g_\beta}{\alpha - \beta} \right)^{\Delta t_j} \right]$$

where Δt_j is in years. For the exponential model (used in the base case) the expected increment is

(29) $$\hat{d}_j = \Delta t_j g_\alpha \left(g_\beta / g_\alpha \right)^{(L_j - \alpha)/(\beta - \alpha)}$$

The error around an expected increment is:

(30) $$\sigma_j^{\,d} = \left(\hat{d}_j \phi - \sigma_{MIN} \right) \left(\frac{1}{\pi} \tan^{-1} \left(10^6 \left(\hat{d}_j \phi - \sigma_{MIN} \right) \right) + 0.5 \right) + \sigma_{MIN}$$

Predicted maturity-at-length is:

(31) $$\hat{p}^{mat}_k = \frac{1}{1 + 19^{-\left((l_k - L_{50}) / L_{95-50} \right)}}$$

2.1.8 Fitting

2.1.8.1 Likelihoods

The distribution of CPUE is assumed to be normal-log and the negative log-likelihood is:

(32) $$-\ln(\mathbf{L})\left(\hat{I}_t \mid \theta \right) = \frac{\left(\ln(I_t) - \ln\left(\hat{I}_t \right) \right)^2}{2\left(\sigma_t^I \tilde{\sigma} / \varpi^I \right)^2} + \ln\left(\sigma_t^I \tilde{\sigma} / \varpi^I \right) + 0.5 \ln(2\pi)$$

and similarly for PCPUE:

(33) $$-\ln(\mathbf{L})\left(\hat{I}2_t \mid \theta\right) = \frac{\left(\ln\left(I2_t\right) - \ln\left(\hat{I}2_t\right)\right)^2}{2\left(\sigma_t^{I2}\tilde{\sigma}\,/\,\varpi^{I2}\right)^2} + \ln\left(\sigma_t^{I2}\tilde{\sigma}\,/\,\varpi^{I2}\right) + 0.5\ln\left(2\pi\right)$$

The distribution of the RDSI is also assumed to be normal-log and the negative log-likelihood is:

(34) $$-\ln(\mathbf{L})\left(\hat{J}_t \mid \theta\right) = \frac{\left(\ln\left(J_t\right) - \ln\left(\hat{J}_t\right)\right)^2}{2\left(\sigma_t^{J}\tilde{\sigma}\,/\,\varpi^{J}\right)^2} + \ln\left(\sigma_t^{J}\tilde{\sigma}\,/\,\varpi^{J}\right) + 0.5\ln\left(2\pi\right)$$

The proportions-at-length from CSLF data are assumed to follow a multinomial distribution, with a standard deviation that depends on the effective sample size (see section 2.2.9.3) and the weight assigned to the data:

(35) $$\sigma_{k,t}^{s} = \frac{\widetilde{\sigma}}{\varpi^{s} n_t^{s}}$$

The negative log-likelihood is:

(36) $$-\ln(\mathrm{L})\left(\hat{p}_{k,t}^{s} \mid \theta\right) = \frac{p_{s,t}^{s}}{\sigma_{k,t}^{s}}\left(\ln\left(p_{k,t}^{s} + 0.01\right) - \ln\left(\hat{p}_{k,t}^{s} + 0.01\right)\right)$$

The likelihood for research diver sampling is analogous. Errors in the tag-recapture dataset were also assumed to be normal. For the *j*th record, the total error is a function of the predicted standard deviation (equation (30)), observation error, and weight assigned to the data:

(37) $$\sigma_j^{tag} = \tilde{\sigma} / \varpi^{tag}\sqrt{{\sigma_{obs}}^2 + \left(\sigma_j^{\,d}\right)^2}$$

and the negative log-likelihood is:

(38) $$-\ln(\mathbf{L})\left(\hat{d}_j \mid \theta\right) = \frac{\left(d_j - \hat{d}_j\right)^2}{2\left(\sigma_j^{tag}\right)^2} + \ln\left(\sigma_j^{tag}\right) + 0.5\ln\left(2\pi\right)$$

The proportion mature-at-length was assumed to be normally distributed, with standard deviation analogous to proportions-at-length:

(39) $$\sigma_k^{mat} = \frac{\tilde{\sigma}}{\varpi^{mat}\sqrt{p_k^{mat} + 0.1}}$$

The negative log-likelihood is:

(40) $$-\ln(\mathbf{L})\left(\hat{p}_k^{mat} \mid \theta\right) = \frac{\left(p_k^{mat} - \hat{p}_k^{mat}\right)^2}{2\left(\sigma_k^{mat}\right)^2} + \ln\left(\sigma_k^{mat}\right) + 0.5\ln\left(2\pi\right)$$

2.1.8.2 Normalised residuals

These are calculated as the residual divided by the relevant σ term used in the likelihood. For CPUE, the normalised residual is

$$(41) \qquad \frac{\ln\left(I_t\right)-\ln\left(\hat{I}_t\right)}{\left(\sigma_t^I \tilde{\sigma} \Big/ \varpi^I\right)}$$

and similarly for PCPUE and RDSI. For the CSLF proportions-at-length, the residual is:

$$(42) \qquad \frac{p_{k,t}^s-\hat{p}_{k,t}^s}{\sigma_{k,t}^s}$$

and similarly for proportions-at-length from the RDLFs. Because the vectors of observed proportions contain many empty bins, the residuals for proportions-at-length include large numbers of small residuals, which distort the frequency distribution of residuals. When presenting normalised residuals from proportions-at-length, we arbitrarily ignore normalised residuals less than 0.05.

For tag-recapture data, the residual is:

$$(43) \qquad \frac{d_j-\hat{d}_j}{\sigma_j^{tag}}$$

and for the maturity-at-length data the residual is:

$$(44) \qquad \frac{p_k^{mat}-\hat{p}_k^{mat}}{\sigma_k^{mat}}$$

2.1.8.3 Dataset weights

Proportions at length (CSLF and RDLF) were included in the model with a multinomial likelihood. The length frequencies for individual years were assigned relative weights (effective sample size), based on a sample size that represented the best least squares fit of $\log(cv_i)$~$\log(P_i)$, where cv_i was the bootstrap c.v. for the ith proportion, P_i. (See Figure A1, Appendix A, for a plot of this relationship). The weights for individual years (n_t^s for CSLF and n_t^r for RDLF) were multiplied by the weight assigned to the dataset (ϖ_s for CSLF and ϖ_r for RDLF) to obtain the model weights for the observations.

In previous assessments, the weight of the dataset was determined iteratively so that the standardised deviation of the normalised residuals was close to one. In this assessment, we explored an alternative weighting scheme following Francis (2011), where the weight for the CSLF dataset was determined as

$$(45) \qquad \varpi^s = 1/\operatorname{var}_t\left[\left(\overline{O}_t^s-\overline{E}_t^s\right)/\left(v_t^s/n_t^s\right)^{0.5}\right] \quad \text{(Method TA1.8, Table A1 in Francis 2011)}$$

Where

(46) $$\overline{O}_t^s = \sum_k p_{k,t}^s l_k$$

(47) $$\overline{E}_t^s = \sum_k \hat{p}_{k,t}^s l_k$$

(48) $$v_t^s = \sum_k (l_k)^2 \hat{p}_{k,t}^s - \left(\overline{E}_t^s\right)^2$$

The weight for the RDLF dataset was calculated similarly. This weighting method allows for the possibility of substantial correlations within a dataset, and generally produces relatively smaller sample size, thus down-weighting the composition data (Francis 2011). The actual and estimated sample sizes for the commercial catch and research diver proportions at length are given in

Table 1 and Table 2.

.

2.1.8.4 Priors and bounds

Bayesian priors were established for all estimated parameters (Table 3). Most were incorporated simply as uniform distributions with upper and lower bounds set arbitrarily wide so as not to constrain the estimation. The prior probability density for M was a normal-log distribution with mean μ_M and standard deviation σ_M . The contribution to the objective function of estimated $M = x$ is:

$$(49) \qquad -\ln(\mathbf{L})(x \mid \mu_M, \sigma_M) = \frac{\left(\ln(M) - \ln(\mu_M)\right)^2}{2{\sigma_M}^2} + \ln\left(\sigma_M \sqrt{2\pi}\right)$$

The prior probability density for the vector of estimated recruitment deviations ε , was assumed to be normal with a mean of zero and a standard deviation of 0.4. The contribution to the objective function for the whole vector is:

$$(50) \qquad -\ln(\mathbf{L})(\varepsilon \mid \mu_\varepsilon, \sigma_\varepsilon) = \frac{\sum_{i=1}^{n_\varepsilon} (\varepsilon_i)^2}{2{\sigma_\varepsilon}^2} + \ln(\sigma_\varepsilon) + 0.5\ln(2\pi).$$

Constant parameters are given in**Error! Reference source not found.**

2.1.8.5 Penalty

A penalty is applied to exploitation rates higher than the assumed maximum (equation 12); it is added to the objective function after being multiplied by an arbitrary weight (1E6) determined by experiment.

AD Model Builder™ also has internal penalties that keep estimated parameters within their specified bounds, but these should have no effect on the final outcome, because choice of a base case excludes the situations where parameters are estimated at or near a bound.

2.1.9 Fishery indicators

The assessment calculates the following quantities from their posterior distributions: the model's mid-season spawning and recruited biomass for 2011 ($B_{current}$ and $B^r_{current}$) and for the projection period (B_{proj} and B^r_{proj}), and from a reference period from 1985 to 1987. The means of values from the three years were called B_{ref} and B^r_{ref} for spawning and recruited biomass respectively.

In the 2010 assessment for PAU 5A, Fu & McKenzie (2010a, 2010b) reported B_{init} ; the spawning stock biomass at the end of the initialisation phase (the equilibrium biomass assuming that recruitment is equal to base recruitment and with no fishing), and B_0 ; the equilibrium spawning stock biomass assuming that recruitment is equal to the average recruitment from the period for which recruitment deviations were estimated (B_0 normally differs from B_{init}). In this assessment a constraint was placed on the recruitment deviations so that their average is 1 for the period in which they are estimated, based on the parameterisation of Bull et al (2012. This ensures that the average recruitment for the period in which they are estimated (1980–2008) is close to R_0 , and as a result B_{init} will be close to B_0 . This assessment also reports the following fishery indictors:

$\%B_0$	Ratio of current and projected spawning biomass to B_0
$\%B_{ref}$	Ratio of current and projected spawning biomass to B_{ref}
$\Pr(> B_{ref})$	Probability that current and projected spawning biomass greater than B_{ref}
$\Pr(> B_{current})$	Probability that projected spawning biomass greater than $B_{current}$
$\%B_0^r$	Ratio of current and projected recruited biomass to B_0^r
$\%B_{ref}^r$	Ratio of current and projected recruited biomass to B_{ref}^r
$\Pr(> B_{ref}^r)$	Probability that current and projected recruit-sized biomass greater than B_{ref}^r
$\Pr(> B_{current}^r)$	Probability that projected recruit-sized biomass greater than $B_{current}^r$
$\Pr(B_{proj} < 20\%B_{ref})$	Probability that projected spawning biomass less than 20% B_0
$\Pr(B_{proj} < 10\%B_{ref})$	Probability that projected spawning biomass less than 10% B_0

2.1.10 Markov chain-Monte Carlo (MCMC) procedures

AD Model Builder™ uses the Metropolis-Hastings algorithm. The step size is based on the standard errors of the parameters and their covariance relationships, estimated from the Hessian matrix.

For the MCMCs in this assessment single long chains were run, starting at the MPD estimate. The base case was 5 million simulations long and samples were saved, regularly spaced by 5000. The value of $\tilde{\sigma}$ was fixed to that used in the MPD run because it may be inappropriate to let a variance component change during the MCMC.

2.1.11 Development of base case and sensitivity model runs

To develop the base case, an initial model (0.0) was specified, which included the tag-recapture data from all areas (except for D'Urville), used an exponential growth model, and followed the iterative weighting procedure allowing the SDNRs of each dataset to be close to 1. A number of exploratory runs were subsequently carried out where the following aspects were investigated:

- Subsets of tag-recapture data to be included in the model
- The use of an exponential vs. an inverse-logistic growth model
- Determining the weights of proportion-at-length datasets using the TA1.8 method (see Section 2.1.8.3)
- Whether to exclude the maturity-at-length data from the Northern faces.

The initial model fitted most datasets reasonably well but some issues were raised in the Shellfish Working Group. Firstly, the weights assigned to the proportion-at-length datasets appeared to be high compared to the actual sample size of the observations (See

Table 1 Table 2). Although the length frequency datasets did not have conflicts with the abundance data, they appeared to have some influence on the estimates of the growth. The exploratory run in which tag-recapture data from the Northern faces and Staircase (consisting of mostly slow-growing paua) were removed showed almost no changes to the estimates of growth parameters (Figure A2), and the model was able to fit the subset of tag-recapture data (Perano and Runander) better when the weights of the CSLF and RDLF datasets were substantially reduced or removed (Figure A3). On the other hand, when growth data from all areas were included, the weights of the CSLF and RDLF datasets had very little influence on the estimates of growth (Figure A4). Secondly, the exponential growth model was considered more appropriate than the inverse logistic model as the latter showed more correlations among estimated parameters in this case. Thirdly the inclusion of maturity data from Northern faces produced a much flatter maturity curve (there were more mature paua for the smaller length classes for the Northern faces than for other areas), but had little effect on the estimates of spawning stock biomass.

The Shellfish WG suggested a base case (1.0) in which the tag-recapture data from all areas (except for D'Urville where growth was stunted) were included, growth parameters were estimated within the model using the exponential growth curve, the weighting of the proportion-at-length data was determined using the TA1.8 method, and Maturity data from Northern faces were excluded. The base case also assumed a steepness of 0.75 for the stock- also specified (Table 5). Recruitment relationship and estimated the CPUE shape parameter within the model. Bounds for estimated parameter are given in Table 3 and values for fixed quantities in Table 4. A number of sensitivity runs were Model 1.1 fixed the CPUE shape parameter at 1, assuming a linear relationship between CPUE and abundance. Models 1.2 and 1.3 assumed the stock-recruitment steepness to be 0.5 and 1.0 respectively. Models 1.4 and 1.5 assumed the maximum exploitation rate to be 0.65 and 0.9 respectively. Models 2.0 and 3.0 removed the tag-recapture dataset and fixed the growth parameters at values representing either slow growth ($g_1 = 15$, $g_2 = 5$, and $\varphi = 0.35$) or fast growth ($g_1 = 40$, $g_2 = 8$, and $\varphi = 0.35$), respectively (see Figure A5 in Appendix A for the growth curves used in these model runs).

3. RESULTS

3.1 MPD base case

Model estimates of objective function values (negative log-likelihood), parameters, and indicators for the base case are given in the second column of Table 6. The base case fits the two observed CPUE abundance indices and the RDSI very well (Figure 3) and the model appears to have captured both the trend and inter-annual variations in the three sets of relative abundance indices. Fits to commercial proportions-at-length are very reasonable (Figures 4 and 5) although fits to the left-hand side of the distribution were less adequate between 1990 and 1992. It was noted that the measurement method of total paua length may have been slightly different before 1992 (P.R. Notman, NIWA, pers. comm.). The model slightly underestimated the peak of the commercial length distribution for the recent three years (2008–2010). Fits to the research diver proportions-at-length are reasonable (Figure 5), but there were some misfits to the length distribution for the early years.

QQ plots of the residuals from the fits to the abundance indices show no apparent departure from the normality assumption (Figure 6). For the proportion-at-length data, Francis (2011) suggested that the residuals for individual length classes may not be relevant given the potential correlations in the data, and he suggested using the predicted annual mean length (across length classes) as a diagnostics tool. Figure 7 shows a reasonable match between the predicted and observed mean length for both the CSLF and RDLF. The standard deviations of residuals for the annual mean length were close to unity for both proportion-at-length datasets (see Table 6).

The MPD estimate of M was 0.14, close to the assumed mean of the prior distribution, 0.10. Estimates of growth parameters suggested a mean annual growth of 27.6 mm at 75 mm and 5.5 mm at

120 mm. The estimated growth transition matrix appeared to have accounted for most of the variability in the growth data (Figure 8–left). Estimates of the maturity ogive were sensible, with length at 50% and full maturity estimated to be approximately 90 mm and 112 mm respectively (Figure 8–right). The midpoint of the commercial fishery selectivity was 124.1 mm, just slightly below the MLS, and this ogive was very narrow (see Table 6).The midpoint of the research diver selectivity ogive was about 79 mm, and the ogive was also very steep, with parameter $T_{95\text{-}50}$ estimated be close to the bound of 0.

The MPD estimates for the spawning stock biomass (mature animals) and recruited biomass (animals at or above the MLS) are shown in Figure 9. Both recruited and spawning biomass decreased substantially from 1965, but increased moderately since 2001 (when the voluntary quota shelving took place). The current spawning stock biomass ($B_{current}$) was estimated to be about 22% of B_0 and 65% B_{ref}, and the current recruit-sized biomass ($B^r_{current}$) was about 23% of B^r_0 and 40% B^r_{ref} (see Table 6).

3.2 MPD sensitivity trials

Model estimates of objective function values (negative log-likelihood), parameters, and indicators for sensitivity trials are given in Table 6. A comparison of model fits and estimates between base case and sensitivity runs is shown in Figures A6–A12, Appendix A.

For the sensitivity trials (except for the initial model), the weights of the proportion-at-length data were determined using the TA1.8 method for both the CSLF and RDLF data; for the initial model run (0.0), the weights were determined iteratively, giving SDNRs close to 1 for all datasets (Table 6).

In the initial model, the sample sizes of the CSLF and RDLF datasets were much larger than those in the base case, and this effectively up-weighted the proportion-at-length data relative to the abundance data. As a result the initial model fits the CSLF and RDLF data better than the base case (e.g. the fits were closer to the peaks of the distribution in the recent years for the CSLF, see Figures A6 and A7). However, estimated parameters were very close between the initial model and the base case (see Table 6), and so were the biomass estimates (see the first row in Figure A12).

Fixing the CPUE shape parameter at 1 (model 1.1) had almost no effect on the fits to the CPUE, or on the estimates of abundance (see the second row in Figure A12). This suggested that there was probably very little information in observational data that allowed *h* to be estimated from within the model.

Assuming a lower value (0.5) of the stock-recruitment steepness, model 1.2 produced a higher estimate of *R0* than the base case; with a higher value (1.0) of steepness, model 1.3 produced a lower estimate of *R0*. However, the pattern of estimated recruitment deviations is similar (Figure A10). The models appeared to have compensated for the differences in steepness with changes in *R0*, recruitment deviations, and natural mortality (see Table 6). Estimates of current stock status are fairly similar between these model runs, although there are some differences in the estimated B_0 (see the third row in Figure A12).

In the base case, the maximum exploitation rate (U_{max}) was assumed to be 0.8 and there were two years (2001 and 2003) in which the exploitation rate was estimated to be at the bound (Figure A11). When U_{max} was assumed to be 0.65 (model 1.4), the estimated exploitation rates for 2001 and 2003 were also at the bound; when U_{max} was assumed to be 0.9 (model 1.5), the estimated exploitation rate for 2003 was at the bound. However biomass estimates from these runs were similar (see the fourth row in Figure A12).

When the growth was fixed (fast or slow), the model gave poorer fits to the CSLF and RDLF data (Figures A8 and A9). With the growth parameters fixed at lower values, model 2.0 produced a broader selectivity for the research diver surveys (because there were more, younger, paua in the population). With the growth parameters fixed at higher values, model 3.0 was unable to fit the mode of the commercial length distribution. Biomass estimates were also sensitive to the assumed values of growth (see the fifth row in Figure A12): $B_{current}$ was estimated to be 26% B_0 for model 2.0, or 13% B_0 for model 3.0.

In general, most estimated model parameters were not significantly different among sensitivity trials. Estimates of M ranged from 0.12 to 0.19. Estimates of biomass indicators were sensitive to the assumed growth, but were similar in all other sensitivity trials ($B_{current}$ ranged between 19% and 24%, and $B^r_{current}$ ranged between 8% and 11% B^r_0).

3.3 MCMC results

MCMC simulations were conducted for the base case (1.0) and the initial model (0.0). The main diagnostic used for the MCMC was the trace plots of the posterior samples. In general, the MCMC traces show good mixing for both the base case and the initial model (Figure 10). Some parameters may not have converged (e.g. The traces of α and β show downward trends and that of T_{95-50} shows an upward trend, See Figure 10). However, there is no evidence of non-convergence for the key biomass indicators for both models (Figure 11). There is evidently more variability in the posterior samples for the base case than for the initial model.

The MCMC parameter correlation matrices (Table 7 and 8) show a high correlation between recruitment and *M*, as is usually seen; between the variance parameters of growth and the other two growth parameters, and between the two research diver selectivity parameters. These correlations do not appear to invalidate the models.

3.4 Marginal posterior distributions and the Bayesian fit

For both models , the posteriors for estimated parameters and indicators were generally well formed, and MPDs were mostly near the centres but tended to be below the median of the biomass posterior (Figures 12 and 13). The posteriors for the base case are summarised in Table 9, and for the initial model in Table 10. For the base case, the median of the posterior samples of T_{95-50} deviated from the MPD estimate, which was close to the bound.

For both the base case and initial model, the posteriors of fits to CSLF and RDLF were very reasonable (Figure 14 and 15). The posterior fits to CSLF and RDLF for the base case have much wider ranges than those in the initial model, and this is apparently due to the differences in the weighting of the proportion-at-length data. For the base case the distribution of mean residuals (over the years) have generally centred about zero for both CSLF and RDLF; for the initial model, the residuals appear to have some trends, particularly for the older length classes (Figure 16).

For both models, the posteriors of fits to the abundance indices appear adequate and the predictions encompass the range of the observed values in most years (Figure 17).

The Q-Q plot for the posteriors of the residuals for the fits to the tag-recapture data show a moderately poor fit that is probably related to the influences of proportion-at-length datasets on the growth estimates (Figure 18).

Estimated selectivity for the research diver survey was broad for the base case, and was steep for the initial model (Top panel-Figure 19), possibly due to the inter-annual variability in the length distribution from the research diver surveys, particularly on the left hand side of the distribution in the early years. Posteriors of recruitment deviations exhibited various degrees of variability between the base case and initial model, but the overall pattern was similar (mid panel-Figure 19). Those estimates suggested a period of relatively low recruitment between the late 1990s and the early 2000s. Estimated exploitation rates peaked in 2001 and 2003, but have drastically decreased since then (bottom panel-Figure 19).

The posterior distribution of spawning stock biomass and recruit-sized biomass are shown in Figure 20 for the base case and Figure 21 for the initial model. These estimated biomass trajectories show a rapid decline since the inception of the fishery, followed by a gradual recovery after 2001. The base case suggested that the estimated spawning stock biomass in 2011 ($B_{current}$) was about 22% (19–26%) of B_0, and 66% (56–78%) of B_{ref} and the current recruit-sized biomass ($B^r_{current}$) was about 10% (8–12%) B^r_0 and about 41% (32–54%) of B^r_{ref} (Table 9). The initial model has a similar result, with $B_{current}$ estimated to be about 23% (19–28%) of B_0 and 72% (60–86%) of B_{ref}, and $B^r_{current}$ about 10% (8–13%) of B^r_0 and about 40% (33–48%) of B^r_{ref} (Table 10).

3.5 Projections

Forward projections were evaluated out to 2014 (three years) with each of the posterior samples of estimated parameters, and with assumed future catch and recruitment. Recruitment in projections was obtained by re-sampling the recruitments estimated for 1997 to 2006 – a period with reasonably good estimates of recruitment deviations. Because estimates of recruitments from 2007 onward are poorly determined by the data, the estimated value is inappropriate for projections and was over-written with values obtained by re-sampling. A number of alternative projections were made with different assumptions for the commercial catch: (a) current TACC, (b) 90% of TACC, (c) 85% of TACC, (d) 80% of TACC. Thus the total catches assumed in the projections were (a) 199 716 kg, (b) 180 992 kg, (c) 171 630 kg, and (d) 162 268 kg.

For each of the projections, biomass indicators including the probability of future biomass being greater or less than reference biomass were calculated from the posterior samples. These are summarised in Table 11 to Table 14. The projection assuming current catch level indicates that the median spawning stock biomass will increase slightly, from 22.1% of B_0 in 2011 to 23.4% of B_0 in 2014, and the median recruit-sized biomass will also increase, from 9.8% to 10.5% of B^r_0 (Table 11). Assuming 10%, 15%, and 20% shelving in TACC, the median of B_{2014} will increase to 24.4%, 25.0%, and 25.5% B_0 respectively and the median of B^r_{2014} will increase to 11.7%, 12.3%, and 12.9% of B^r_0 respectively (Table 12–Table 14). The probability of future biomass being greater than the current level also increases with reduced future catches: $\Pr(B_{2014} > B_{current})$ increased from 67% to 90%, and $\Pr(B^r_{2014} > B^r_{current})$ increased from 67% to 99% when the TACC was shelved by up to 20%.

3.6 Assessing the effect of closed areas

The second objective of the report was to assess the potential impact of introducing areas closed to commercial fishing within PAU 7 (area alienation). This was done by running forward projections of the assessment model under scenarios where areas are alienated and catches are displaced.

Three-year projections were carried out, using posterior samples of estimated parameters from the base case, and the proportion alienation is implemented in the model as a proportionate reduction in numbers across all length classes in the first year of closure, and a proportionate reduction in recruitment for the first year of closure and for subsequent years. The proportion alienation for the closed area was estimated from the mean catch from 2006–2010, as a proportion of the total mean catch over the same years. The scenarios modelled here were:

(1) status quo.

(2) implementation of a Tory Channel mataitai (catch displaced to other areas, productivity lost from assessed area)

(3) additional (to 2) reduced catch from D'Urville area because of productivity loss due to quality issues (displaced catch to other areas, productivity lost from assessed area).

(4) additional (to 3) implementation of a west coast mataitai (catch displaced, no productivity loss to assessed area).

The projections were made assuming future catches remained at the current level. For scenarios (3) and (4) additional projections were also carried out assuming 10%, 15%, and 20% shelving of the TACC. The catch and proportion alienation assumed for each of the scenarios are summarised in Table 15.

The projected spawning stock biomass under each scenario is summarised in Table 16, and recruit-sized biomass is summarised in Table 17. Indicators were calculated as the percentage of runs in which future spawning biomass was less than the current level ($\Pr(B_{proj} < B_{curent})$) or future recruit-sized biomass was less than current level ($\Pr(B^r_{proj} < B^r_{current})$).

The projection results show that under all scenarios assuming current TACC, $\Pr(B_{2014} < B_{current})$ and $\Pr(B^r_{2014} < B^r_{current})$ was greater than 50% ($\Pr(B_{2014} < B_{current})$ and $\Pr(B^r_{2014} < B^r_{current})$ was close to 90% or greater for scenarios 3 and 4. If in the future 20% of the TACC was shelved, the probability of future recruit-sized biomass being less than the current level decreases to 41% for scenario 3c, and to 52 % for scenario 4c (see Table 15).

4. DISCUSSION

This report assesses PAU 7 and includes fishery data up to the 2010–11 fishing year. Estimates from the base case model suggested that the current spawning stock population (B_{current}) was 22% (19–26%) B_0, and that the recruit-sized stock abundance ($B^r_{current}$) was 10% (8–12%) of the initial state (B^r_0). The model projections suggested that the stock abundance will increase slightly over the next three years. The projected status of the spawning stock biomass in 2014 is 23.4% (17–35%) of B_0 assuming that the catch remains at its current level, or 25.5% (19–34%) of B_0 assuming a 20% shelving of current TACC.

The model presented, whilst fairly representing the majority of the data, also shows some indications of lack of fit. It is likely that the estimates of historical stock size may not be reliable, given

assumptions about annual recruitment and the use of the historical catch-effort indices of abundance. However, model estimates of recent status generally agree closely with recent CPUE trends.

Fisheries stock assessment models can depend strongly on the relative weights assigned to different datasets (Francis 2011). In the previous PAU 7 assessment the weighting of the observational dataset was determined using an iterative procedure so that the standard deviations of the normalised residuals were close to unity for most datasets. Francis (2011) proposed some weighting methods which account for the correlations in the composition data and which generally produce smaller sample sizes (weights) with these types of data. The main purpose of down-weighing the composition data is to prevent the model from being dominated by that data which may result in a poor fit to the abundance data. However for this assessment, there does not appear to be any major conflict between the abundance (CPUE and RDSI) and the length frequency datasets (CSLF and RDLF), and weights assigned to the CSLF and RDLF do not have a significant impact on fits to the abundance data, although the weighing has apparently influenced the uncertainly of model estimates. In this assessment the proportion-at-length data were down-weighted using the Francis method mainly to reduce their influence on the estimates of growth.

Growth is one of the key parameters that determines the productivity of the stock and was estimated from the annual-increment data in this assessment. For PAU 7, there was some uncertainty in the growth data which showed distinctive growth rates between regions, with paua from the southern areas appearing to grow faster than those from the northern areas. As the weighting of each subarea is defined by the sample size, the combined dataset may not have faithfully represented the average growth of the stock. To evaluate the impact on the assessment due to uncertainty surrounding the growth estimates, it was initially planned to use various subsets of the tag-recapture data to estimate growth. This was not feasible because the estimates of growth were influenced by the proportion-at-length data. Growth rates were therefore fixed at assumed values (fast or slow) in sensitivity trials, loosely based on subsets of the tag-recapture data. Those values were chosen arbitrarily, but were likely to encompass the lower and upper bounds of the true growth. Results from these sensitivity trials suggested that the estimates of stock status were sensitive to the growth rates, and $B_{current}$ ranged between 13% and 26% B_0. However, model fits to observational data were generally poor when these alternative growth rates were used, suggesting that stock status is unlikely to be as extreme as the models suggested. On the other hand, the base case has reasonable fits to most observational data, suggesting that growth estimated using all the tag-recapture data was compatible with other available information about the stock.

In the assessment, the potential impact of introducing areas closed to commercial fishing was assessed via projections in which future recruitments in the closed area were alienated from the rest of the population. This approach was considered to be ad hoc as it is based on the assumption that fishing pressure in the closed and fished areas are the same, and the underlying distribution of the population is proportional to the catch and so is recruitment. The Shellfish WG suggested that a more robust approach would be to conduct a separate assessment of the stock alienating areas closed to commercial fishing. This was not done as it would require a considerable amount of extra work which was considered to be beyond the scope of the present project.

Another limit of the model is that it treats the whole of PAU 7 as if it were a single stock with homogeneous biology, habitat, and fishing pressures. This means the model assumes homogeneity in recruitment, that natural mortality does not vary by size or year, and that growth has the same mean and variance throughout the area (paua fisheries are extremely variable and paua populations can change in very short distances along the coast). Heterogeneity in growth can be a problem for this kind of model (Punt 2003). Variation in growth is addressed to some extent by having a stochastic growth transition matrix based on increments observed in several different places; similarly the length frequency data are integrated across samples from many places. The effect is likely to make model results optimistic. For instance, if some local stocks are fished very hard and others not fished, recruitment failure can result because of the depletion of spawners, because spawners must breed

close to each other and because the dispersal of larvae is unknown. Recruitment failure is a common observation in overseas abalone fisheries, local processes may decrease recruitment, which is an effect that the current model cannot account for.

CPUE provides information on changes of relative abundance. However, CPUE is generally considered to be a poor index of stock abundance for paua, due to divers' ability to maintain catch rates by moving from area to area despite a decreasing biomass (hyperstability). Breen et al. (2003) argued that standardised CPUE might be able to be related to changes of abundance in a fully exploited fishery, and that a large decline in the CPUE is most likely to reflect a decline in the fishery. PAU 7 is generally considered to be a fully developed fishery: the exploitation rate in Statistical Areas 017 and 038 has been high and there are unlikely to be many unfished areas within the stock.

.

Another source of uncertainty is that fishing may cause spatial contraction of populations (e.g., Shepherd & Partington 1995), or that some populations become relatively unproductive after initial fishing (Gorfine & Dixon 2000). If this happens, the model will overestimate productivity in the population as a whole. Past recruitments estimated by the model might instead have been the result of serial depletion. Attempts to estimate the relationship between CPUE and biomass (through the parameter h) have been made in some of the previous paua stock assessments and on some occasions have suggested evidence of hyperstability (McKenzie & Smith. 2009). In this assessment, h was estimated to be between 0.7 and 1 for most model runs, implying a moderate degree of hyperstability. However this may be an artefact of the model as there is little information in the observations that allows h to be estimated.

.

Commercial catch length frequencies provide information on changes in the structure of a population that is under fishing pressure. However, if serial depletion had occurred and fishers had moved from area to area, samples from the commercial catch may not have represented the population of the entire stock. For PAU 7, there has been a long time-series of commercial catch sampling and spatial coverage of samples is generally considered to be adequate throughout the years.

The usefulness of research diver survey indices in providing relative abundance information has been an ongoing concern. Cordue (2009) concluded that the diver survey based on the timed swim approach is fundamentally flawed and is inadequate for providing relative abundance indices. The recent review of survey methodology by Haist (2010) suggested that the existing RDSI data are likely to be more useful at stratum level. The general consensus is the index-abundance relationship from the research diver survey is likely to be nonlinear, and cannot be easily quantified in a stock assessment.

Model fits to the length frequencies from the research diver survey were acceptable, though patterns in residuals were apparent in some years. Cordue (2009) suggested that RDLF are probably more useful at individual stratum level. The RDLF combined across strata may not be able to represent the underlying population at a larger scale as the appropriate weight of individual strata cannot be determined.

Finally, it was not known how well recruitment deviations were estimated. Breen (2003) suggested that the actual recruitment fluctuations could be more extreme than the model suggested, as it takes a few years for paua to recruit into the fishery, and a strong impulse of year-class strengths could cover a wide length range.

5. ACKNOWLEDGMENTS

This work was supported by a contract from the Ministry of Fisheries (PAU2011-06 Objective 1). Thank you to Paul Breen for developing the stock assessment model that was used in this assessment and for the use of major proportions of the 2006 report for this update. Thank you to the Shellfish Working Group for all the advice provided throughout the assessment process.

6. REFERENCES

Andrew, N.L.; Breen, P.A.; Naylor, J.R.; Kendrick, T.H.; Gerring, P. (2000). Stock assessment of paua (*Haliotis iris*) in PAU 7 in 1998–99. *New Zealand Fisheries Assessment Report 2000/49*. 40 p.

Breen, P.A.; Andrew, N.L.; Kendrick, T.H. (2000a). Stock assessment of paua (*Haliotis iris*) in PAU 5B and PAU 5D using a new length-based model. *New Zealand Fisheries Assessment Report 2000/33*. 37 p.

Breen, P.A.; Andrew, N.L.; Kendrick, T.H. (2000b). The 2000 stock assessment of paua (*Haliotis iris*) in PAU 5B using an improved Bayesian length-based model. *New Zealand Fisheries Assessment Report 2000/48*. 36 p.

Breen, P.A.; Andrew, N.L.; Kim, S.W. (2001). The 2001 stock assessment of paua (*Haliotis iris*) in PAU 7. *New Zealand Fisheries Assessment Report 2001/55*. 53 p.

Breen, P.A.; Kim, S.W. (2003). The 2003 stock assessment of paua (*Haliotis iris*) in PAU 7. *New Zealand Fisheries Assessment Report 2003/35.* 112 p.

Breen, P.A.; Kim, S.W. (2004a). The 2004 stock assessment of paua (*Haliotis iris*) in PAU 4. *New Zealand Fisheries Assessment Report 2004/55.* 79 p.

Breen, P.A.; Kim, S.W. (2004b). The 2004 stock assessment of paua (*Haliotis iris*) in PAU 5A. *New Zealand Fisheries Assessment Report 2004/40*. 86 p.

Breen, P.A.; Kim, S.W. (2005). The 2005 stock assessment of paua (*Haliotis iris*) in PAU 7. *New Zealand Fisheries Assessment Report 2005/47.* 114 p.

Breen, P.A.; Kim, S.W. (2007). The 2006 stock assessment of paua (*Haliotis iris*) stocks PAU 5A (Fiordland) and PAU 5D (Otago). *New Zealand Fisheries Assessment Report 2007/09*. 164 p.

Breen, P.A.; Kim, S.W.; Andrew, N.L. (2003). A length-based Bayesian stock assessment model for abalone. *Marine and Freshwater Research 54(5):* 619–634.

Bull, B.; Francis, R.I.C.C.; Dunn, A.; McKenzie, A.; Gilbert, D.J.; Smith, M.H.; Bian, R. (2012). CASAL (C++ algorithmic stock assessment laboratory): CASAL User Manual v2.30-2012/03/21. NIWA Technical Report 135.

Cordue, P.L. (2009). Analysis of PAU5A dive survey data and PCELR catch and effort data. Final report for SeaFIC and PauaMAC5. (Unpublished report held by SeaFIC.)

Francis, R.I.C.C. (2011). Data weighting in statistical fisheries stock assessment models. *Canadian Journal of Fisheries and Aquatic Sciences* 68: 15.

Fu, D.; McKenzie, A; Naylor, R. (2012). Summary of input data for the 2011 PAU 7 stock assessment. *New Zealand Fisheries Assessment Report 2012/26* 46 p.

Fu, D.; McKenzie, A. (2010a). The 2010 stock assessment of paua (*Haliotis iris*) for Chalky and South Coast in PAU 5A. *New Zealand Fisheries Assessment Report 2010/36.* 63 p.

Fu, D.; McKenzie, A. (2010b). The 2010 stock assessment of paua (*Haliotis iris*) for Milford, George, Central, and Dusky in PAU 5A. *New Zealand Fisheries Assessment Report 2010/46*. 55 p.

Gorfine, H.K.; Dixon, C.D. (2000). A behavioural rather than resource-focused approach may be need to ensure sustainability of quota managed abalone fisheries. *Journal of Shellfish Research* 19: 515–516.

Haist, V. (2010). Paua research diver survey: review of data collected and simulation study of survey method. *New Zealand Fisheries Assessment Report 2010/38*. 54 p.

Kim, S.W.; Bentley, N.; Starr, P.J.; Breen, P.A. (2004). Assessment of red rock lobsters (*Jasus edwardsii*) in CRA 4 and CRA 5 in 2003. *New Zealand Fisheries Assessment Report 2004/8.* 165 p.

McShane, P.E.; Mercer, S.F.; Naylor, J.R. (1994). Spatial variation and commercial fishing of the New Zealand paua (*Haliotis iris* and *H. australis*). *New Zealand Journal of Marine and Freshwater Research* 28: 345–355.

McShane, P.E.; Mercer, S.; Naylor, J.R.; Notman, P.R. (1996): Paua (*Haliotis iris*) fishery assessment in PAU 5, 6, and 7. New Zealand Fisheries Assessment Research Document 96/11. 35 p. (Unpublished report held in NIWA library, Wellington.)

McKenzie, A.; Smith, A.N.H. (2009). The 2008 stock assessment of paua (*Haliotis iris*) in PAU 7. *New Zealand Fisheries Assessment Report 2009/34.* 84 p.

Punt, A.E. (2003). The performance of a size-structured stock assessment method in the face of spatial heterogeneity in growth. *Fisheries Research 65:* 391–409.

Schiel, D.R. (1989). Paua fishery assessment 1989. New Zealand Fisheries Assessment Research Document 89/9: 20 p. (Unpublished report held in NIWA library, Wellington, New Zealand.)

Schiel, D.R. (1992). The paua (abalone) fishery of New Zealand. *In:* Abalone of the world: Biology, fisheries and culture. Shepherd, S.A.; Tegner, M.J.; Guzman del Proo, S. (eds.) pp. 427–437. Blackwell Scientific, Oxford.

Schiel, D.R.; Breen, P.A. (1991). Population structure, ageing and fishing mortality of the New Zealand abalone *Haliotis iris*. *Fishery Bulletin 89*: 681–691.

Shepherd, S.A.; Breen, P.A. (1992). Mortality in abalone: its estimation, variability and causes. *In*: 'Abalone of the World: Biology, Fisheries and Culture'. (Eds S.A. Shepherd, M.J. Tegner, and S. Guzman del Proo.) pp. 276–304. (Blackwell Scientific: Oxford.)

Shepherd, S.A.; Partington, D. (1995). Studies on Southern Australian abalone (genus Haliotis). XVI. Recruitment, habitat and stock relations. *Marine and Freshwater Research 46*: 669–680.

Shepherd, S.A.; Rodda, K.R.; Vargas, K.M. (2001). A chronicle of collapse in two abalone stocks with proposals for precautionary management. *Journal of Shellfish Research 20:* 843–856.

Table 1: Actual sample sizes, effective sample sizes determined for the multinomial likelihood, and model weighted sample sizes (for Models 0.0 and 1.0) for the PAU 7 commercial catch sampling length frequencies for 1990–1994 and 1999–2009.

Fishing year	Actual sample size	Effective sample size	Initial model (0.0) sample size	Base case (1.0) sample size
1990	4 726	910	319	55
1991	9 577	1 245	436	75
1992	8 759	949	332	57
1993	7 960	1 191	417	71
1994	8 752	1 958	685	117
1999	5 199	929	325	56
2000	5 382	1 307	457	78
2001	3 466	969	339	58
2002	6 418	1 590	557	95
2003	6 608	1 664	582	100
2004	4 304	1 419	497	85
2005	4 022	1 203	421	72
2006	2 641	757	265	45
2007	5 466	1 373	481	82
2008	9 354	1 645	576	99
2009	5 477	1 282	449	77
2010	10 748	2 590	907	155

Table 2: Actual sample sizes, effective sample sizes determined for the multinomial likelihood, and model weighted sample sizes (for Models 0.0 and 1.0) for the PAU 7 research diver length frequencies for 1990, 1993, 1995, 1996, 1999, 2001, 2003, and 2005.

Fishing year	Actual sample size	Effective sample size	Initial model (0.0) sample size	Base case (1.0) sample size
1990	2440	779	2571	39
1993	3609	510	1683	26
1995	3416	244	805	12
1996	3574	362	1195	18
1999	5675	573	1891	29
2001	4349	1044	3445	52
2003	4674	1653	5455	83
2005	4999	1373	4531	69

Table 3: Base case model specifications: for estimated parameters, the phase of estimation, type of prior, (U, uniform; N, normal; LN, lognormal), mean and c.v. of the prior, lower bound and upper bound.

Parameter	Phase	Prior	μ	c.v.	Bounds	
					Lower	Upper
ln($R0$)	1	U	–	–	5	50
M	3	LN	0.1	0.35	0.01	0.5
g_1	2	U	–	–	1	50
$g2$	2	U	–	–	0.01	50
φ	2	U	–	–	0.001	1
$Ln(q^I)$	1	U	–	–	-30	0
$Ln(q^J)$	1	U	–	–	-30	0
$Ln(q^k)$	1	U	–	–	-30	0
L_{50}	1	U	–	–	70	145
L_{95-50}	1	U	–	–	1	50
T_{50}	2	U	–	–	70	125
T_{95-50}	2	U	–	–	0.001	50
D_{50}	2	U	–	–	70	145
D_{95-50}	2	U	–	–	0.01	50
[illegible]	1	N	0	0.4	-2.3	2.3
h	1	U	–	–	0.01	2

Table 4: Values for fixed quantities for base case model.

Variable	Value
L_1	75
L_2	120
a	2.59E-08
b	3.322
U^{max}	0/80
σ_{min}	1
σ_{obs}	0.25
$\tilde{\sigma}$	0.2
H	0.75

Table 5: Summary descriptions for base case and sensitivity model runs.

Model runs	Description
0.0 (Initial model)	Iterative reweighting, assumed H of 0.75 and U^{max} of 0.8, estimated h
1.0 (Base case)	TA1.8 weighting method, assumed H of 0.75 and U^{max} of 0.8, estimated h
1.1	1.0, but fixed CPUE shape parameter (h) at 1
1.2	1.0, but assuming steepness (H) of 1
1.3	1.0, but assuming steepness (H) of 0.5
1.4	1.0, but assuming maximum exploitation rate (U^{max}) of 0.9
1.5	1.0, but assuming maximum exploitation rate (U^{max}) of 0.65
2.0	1.0, fixing growth parameters ($g_1 = 15$, $g_2 = 5$, and $\varphi = 0.35$)
3.0	1.0, fixing growth parameters ($g_1 = 40$, $g_2 = 8$, and $\varphi = 0.35$)

Table 6: MPD estimates for base case and sensitivity trials. Shading indicates parameter fixed and likelihood contributions not used when datasets were removed. SDNRs for CSLF and RDLF were calculated from mean length for runs using TA.18 weighting method.

Model runs	0.0	1.0	1.1	1.2	1.3	1.4	1.5	2.0	3.0
Likelihoods									
CPUE	-17.6	-21.8	-14.6	-21.8	-21.5	-22.2	-19.2	-19.9	-17.9
RDSI	-1.6	-2.8	-2.8	-3.2	-2.6	-2.1	-3.3	-2.1	0.4
CSLF	214.6	23.1	31.0	29.0	17.4	19.0	33.2	19.2	126.1
RDLF	195.4	8.4	7.7	7.7	11.0	7.6	9.7	6.2	24.3
Tags	1186.4	1176.6	1176.1	1175.8	1178.1	1173.5	1180.0	1215.2	1255.1
Maturity	-30.6	-30.6	-30.6	-30.6	-30.6	-30.6	-30.6	-30.6	-30.6
PCPUE	-9.1	-12.0	-17.1	-12.1	-11.7	-12.5	-10.0	-10.8	-9.0
Prior on M	3.4	4.5	6.8	0.2	16.9	5.5	4.2	3.2	57.4
Prior on ε	15.6	4.4	3.9	3.0	9.3	3.5	3.7	2.7	12.6
U penalty	0.09	0.01	0.00	0.01	0.00	0.00	0.08	0.00	1.28
ε penalty	0.00	0.00	0.00	0.00	0.00	0.00	0.00	0.00	0.00
Total	1556.5	1149.7	1160.4	1148.0	1166.2	1141.5	1167.8	-32.3	164.4
Parameters									
ln($R0$)	14.5	14.5	14.5	14.2	15.0	14.5	14.5	14.7	14.4
M	0.136	0.141	0.150	0.119	0.183	0.145	0.139	0.135	0.172
L_{50}	90.7	90.7	90.7	90.7	90.7	90.7	90.7	90.7	90.7
$L_{95\text{-}50}$	11.4	11.4	11.4	11.4	11.4	11.4	11.4	11.4	11.5
D_{50}	124.2	124.1	124.2	124.1	124.2	124.2	124.0	124.3	123.3
$D_{95\text{-}50}$	2.7	2.6	2.7	2.6	2.7	2.6	2.5	2.8	2.1
T_{50}	79.1	79.4	79.1	80.1	79.0	99.4	79.3	108.9	79.0
$T_{95\text{-}50}$	0.1	0.3	0.1	0.9	0.0	22.4	0.3	26.5	0.0
ln(q^{I})	-9.6	-9.7	-13.1	-10.5	-8.9	-9.1	-11.7	-10.6	-11.1
ln(q^{I2})	-9.0	-9.2	-12.4	-9.9	-8.3	-8.5	-11.2	-10.0	-10.5
ln(q^{J})	-15.4	-15.4	-15.4	-15.3	-15.5	-15.2	-15.5	-15.3	-14.7
h	0.73	0.74	1.00	0.80	0.67	0.70	0.88	0.80	0.86
g_{α}	29.1	27.6	27.3	27.3	27.9	24.3	27.7	15.0	40.0
g_{β}	4.8	5.5	5.5	5.6	5.4	5.8	5.2	5.0	8.0
α	0.91	0.83	0.83	0.81	0.88	0.93	0.85	0.35	0.35
β	0.79	0.78	0.78	0.79	0.76	0.78	0.76	1.00	1.00
Indicators									
B_0	4152	4156	3927	3916	4700	4112	4181	4566	3640
B_{ref}	1310	1359	1285	1230	1660	1343	1437	1823	832
$B_{current}$	902	877	826	870	905	836	996	1204	461
$B_{current} / B_0$	0.22	0.21	0.21	0.22	0.19	0.20	0.24	0.26	0.13
$B_{current} / B_{ref}$	0.69	0.65	0.64	0.71	0.55	0.62	0.69	0.66	0.55
B_0^r	3343	3368	3124	3310	3475	3310	3328	3388	3268
B_{ref}^r	734	777	640	671	976	748	777	831	564
$B_{current}^r$	310	313	261	304	318	269	365	352	241

$B^r_{current} / B^r_0$	0.09	0.09	0.08	0.09	0.09	0.08	0.11	0.10	0.07
$B^r_{current} / B^r_{ref}$	0.42	0.40	0.41	0.45	0.33	0.36	0.47	0.42	0.43
$U_{current}$	0.43	0.43	0.49	0.44	0.43	0.48	0.38	0.39	0.53
Weights									
CPUE	0.06	0.06	0.04	0.06	0.06	0.06	0.05	0.05	0.10
RDSI	0.11	0.10	0.10	0.11	0.10	0.09	0.12	0.11	0.09
CSLF	0.07	0.01	0.01	0.01	0.01	0.01	0.01	0.01	0.02
RDLF	0.67	0.01	0.01	0.01	0.02	0.01	0.02	0.01	0.02
Tags	0.18	0.18	0.18	0.18	0.18	0.20	0.17	0.08	0.15
Maturity	4.27	4.27	4.27	4.27	4.27	4.27	4.27	4.27	4.27
PCPUE	0.06	0.06	0.10	0.06	0.06	0.06	0.05	0.05	0.10
SDNRs									
CPUE	1.01	0.76	0.73	0.76	0.78	0.73	0.70	0.64	1.42
RDSI	1.04	0.75	0.75	0.80	0.79	0.74	0.88	0.97	1.12
CSLF	0.94	0.99	0.97	1.03	0.95	1.00	0.90	1.03	1.06
RDLF	0.99	0.99	1.01	0.96	1.08	1.00	1.01	1.02	1.00
Tags	0.99	1.02	1.02	1.02	1.03	1.01	1.03	0.87	0.89
Maturity	1.00	1.00	1.00	1.00	1.00	1.00	1.00	1.00	1.00
PCPUE	1.03	0.69	0.70	0.68	0.73	0.61	0.72	0.59	1.45

Table 7: Correlations among estimated parameters for the MCMC 1.0.

	$\ln(R0)$	M	g_α	g_β	L_{50}	$L_{95\text{-}50}$	D_{50}	$D_{95\text{-}50}$	T_{50}	$T_{95\text{-}50}$	α	β	$\ln(q^{I})$	$\ln(q^{I2})$	$\ln(q^{J})$	h
$\ln(R0)$	1.00															
M	0.89	1.00														
g_α	-0.25	0.00	1.00													
g_β	0.13	0.36	-0.19	1.00												
L_{50}	0.00	0.00	0.00	0.00	1.00											
$L_{95\text{-}50}$	0.00	0.00	0.00	0.00	1.00	1.00										
D_{50}	0.13	0.04	-0.07	-0.25	0.00	0.00	1.00									
$D_{95\text{-}50}$	0.07	0.04	0.00	-0.12	0.00	0.00	0.52	1.00								
T_{50}	0.01	0.00	0.00	0.00	0.00	0.00	0.00	0.00	1.00							
$T_{95\text{-}50}$	0.00	0.00	0.00	0.00	0.00	0.00	0.00	0.00	-0.45	1.00						
α	-0.02	-0.19	0.03	-0.50	0.00	0.00	0.17	0.06	0.00	0.00	1.00					
β	0.02	0.16	-0.06	0.35	0.00	0.00	-0.16	-0.05	0.00	0.00	-0.95	1.00				
$\ln(q^{I})$	-0.38	-0.50	0.03	-0.05	0.00	0.00	-0.04	-0.02	0.00	0.00	0.00	0.01	-0.02			
$\ln(q^{I2})$	-0.41	-0.52	0.03	-0.05	0.00	0.00	-0.05	-0.02	0.00	0.00	0.01	0.00	-0.01	1.00		
$\ln(q^{J})$	-0.21	-0.01	0.38	0.22	0.00	0.00	-0.20	-0.08	0.00	0.00	-0.25	0.23	-0.06	0.07	1.00	
h	0.41	0.52	-0.03	0.06	0.00	0.00	0.05	0.03	0.00	0.00	-0.01	0.00	0.01	-1.00	-0.06	1.00

Table 8: Correlations among estimated parameters for the MCMC 0.0.

	$\ln(R0)$	M	g_α	g_β	L_{50}	$L_{95\text{-}50}$	D_{50}	$D_{95\text{-}50}$	T_{50}	$T_{95\text{-}50}$	α	β	$\ln(q^{I})$	$\ln(q^{I2})$	$\ln(q^{J})$	h
$\ln(R0)$	1.00															
M	0.91	1.00														
g_α	0.14	0.22	1.00													
g_β	0.02	0.21	-0.36	1.00												
L_{50}	0.00	0.00	0.00	0.00	1.00											
$L_{95\text{-}50}$	0.00	0.00	0.00	0.00	1.00	1.00										
D_{50}	0.03	-0.09	-0.08	-0.29	0.00	0.00	1.00									
$D_{95\text{-}50}$	0.02	-0.04	-0.02	-0.15	0.00	0.00	0.54	1.00								
T_{50}	0.01	0.01	0.00	0.00	0.00	0.00	0.00	0.00	1.00							
$T_{95\text{-}50}$	0.00	0.00	0.00	0.00	0.00	0.00	0.00	0.00	-0.45	1.00						
α	-0.17	-0.27	0.38	-0.57	0.00	0.00	0.30	0.11	0.00	0.00	1.00					
β	0.20	0.25	-0.41	0.30	0.00	0.00	-0.26	-0.10	0.00	0.00	-0.93	1.00				
$\ln(q^{I})$	-0.13	-0.30	-0.04	-0.10	0.00	0.00	0.01	0.00	0.00	0.00	0.08	-0.07	-0.06			
$\ln(q^{I2})$	-0.16	-0.31	-0.05	-0.09	0.00	0.00	0.02	0.00	0.00	0.00	0.08	-0.08	-0.07	1.00		
$\ln(q^{J})$	-0.03	0.04	0.04	0.14	0.00	0.00	-0.15	-0.08	0.00	0.00	-0.12	0.10	-0.02	-0.01	1.00	
h	0.14	0.31	0.04	0.10	0.00	0.00	-0.01	0.00	0.00	0.00	-0.08	0.07	0.06	-1.00	0.02	1.00

Table 9 : Summary of the marginal posterior distributions from the MCMC chain from the base case (1.0). The columns show the minimum values observed in the 1000 samples, the maxima, the 5th and 95th percentiles, and the medians. Biomass is in tonnes.

	Min	5%	Median	95%	Max	MPD estimate
Parameters						
f	1159.2	1164.2	1170.9	1178.9	1191.4	1149.7
ln(*R0*)	14.4	14.4	14.5	14.6	14.7	14.5
M	0.115	0.127	0.139	0.154	0.172	0.141
T_{50}	79.1	82.7	94.6	103.1	111.7	79.4
$T_{95\text{-}50}$	0.0	3.7	15.4	23.0	32.1	0.3
D_{50}	123.3	123.7	124.1	124.4	124.7	124.1
$D_{95\text{-}50}$	0.8	1.9	2.6	3.2	3.8	2.6
L_{50}	88.7	89.9	90.7	91.4	92.2	90.7
$L_{95\text{-}50}$	8.3	9.8	11.6	13.4	15.7	11.4
$\ln(q^{I})$	-14.0	-11.4	-9.7	-8.4	-7.2	-9.7
$\ln(q^{II})$	-13.1	-10.8	-9.1	-7.9	-6.6	-9.2
$\ln(q^{J})$	-15.7	-15.5	-15.3	-15.1	-14.9	-15.4
g_{α}	20.8	23.0	25.8	28.7	32.1	27.6
g_{β}	4.6	5.1	5.5	5.8	6.3	5.5
α	0.57	0.68	0.86	1.05	1.33	0.83
β	0.61	0.70	0.79	0.88	0.99	0.78
h	0.54	0.63	0.73	0.87	1.06	0.74
Indicators						
B_0	3608	3905	4242	4541	4888	4156
B_{ref}	1158	1299	1426	1561	1726	1359
$B_{current}$	638	790	933	1115	1317	877
$B_{current}/B_0$	0.14	0.19	0.22	0.26	0.32	0.21
$B_{current}/B_{ref}$	0.47	0.56	0.66	0.78	0.91	0.65
B_0^r	2772	3063	3417	3719	4000	3368
B_{ref}^r	514	669	816	971	1161	777
$B_{current}^r$	199	261	334	428	571	313
$B_{current}^r/B_0^r$	0.06	0.08	0.10	0.12	0.17	0.09
$B_{current}^r/B_{ref}^r$	0.24	0.32	0.41	0.54	0.73	0.40
$U_{current}$	0.27	0.33	0.41	0.49	0.59	0.43

Table 10: Summary of the marginal posterior distributions from the MCMC chain from the initial model (0.0). The columns show the minimum value of each parameter observed in the 1000 samples, the 5th percentile, the median, the 95th percentile, the maximum, and the MPD estimate. Biomass is in tonnes.

	Minimum	5%	Median	95%	Maximum	MPD estimate
Parameters						
F	1563.0	1570.1	1577.0	1585.5	1596.3	1556.5
ln(*R0*)	14.4	14.5	14.5	14.6	14.6	14.5
M	0.119	0.127	0.135	0.145	0.157	0.136
T_{50}	79.0	79.3	80.1	81.1	83.4	79.1
$T_{95\text{-}50}$	0.0	0.2	0.9	1.6	3.5	0.1
D_{50}	124.0	124.1	124.2	124.4	124.5	124.2
$D_{95\text{-}50}$	2.3	2.5	2.7	2.9	3.3	2.7
L_{50}	88.8	89.9	90.7	91.5	92.2	90.7
$L_{95\text{-}50}$	8.2	9.9	11.5	13.5	15.7	11.4
$\ln(q^{I})$	-11.9	-10.6	-9.5	-8.3	-7.0	-9.6
$\ln(q^{II})$	-11.2	-10.0	-8.9	-7.8	-6.7	-9.0
$\ln(q^{J})$	-15.7	-15.5	-15.4	-15.3	-15.0	-15.4
g_{α}	27.1	28.1	29.2	30.4	31.7	29.1
g_{β}	3.9	4.3	4.6	4.9	5.2	4.8
α	0.65	0.80	0.98	1.20	1.40	0.91
β	0.66	0.71	0.78	0.85	0.93	0.79
h	0.53	0.63	0.72	0.80	0.90	0.73
Indicators						
B_0	3716	3960	4171	4369	4584	4152
B_{ref}	1200	1271	1341	1419	1523	1310
$B_{current}$	668	803	960	1172	1476	902
$B_{current}/B_0$	0.16	0.19	0.23	0.28	0.35	0.22
$B_{current}/B_{ref}$	0.51	0.60	0.72	0.86	1.03	0.69
B_0^r	2898	3129	3338	3535	3731	3343
B_{ref}^r	608	674	740	810	929	734
$B_{current}^r$	187	265	336	432	550	310
$B_{current}^r/B_0^r$	0.06	0.08	0.10	0.13	0.17	0.09
$B_{current}^r/B_{ref}^r$	0.26	0.36	0.46	0.58	0.75	0.42
$U_{current}$	0.27	0.33	0.40	0.48	0.61	0.43

Table 11: Summary of key indicators from the projection for the base case MCMC with future commercial catch set to current TACC: projected biomass as a percentage of the virgin and current stock status, for spawning stock and recruit-sized biomass, respectively.

Projection under current TACC	2011	2012	2013	2014
$\%B_0$	0.221 (0.180–0.272)	0.225 (0.175–0.284)	0.229 (0.171–0.300)	0.234 (0.165–0.315)
$\%B_{ref}$	0.655 (0.537–0.805)	0.667 (0.528–0.840)	0.681 (0.513–0.893)	0.693 (0.494–0.942)
$\Pr(> B_{ref})$	0.000	0.000	0.001	0.008
$\Pr(> B_{current})$		0.592	0.637	0.671
$\Pr(< 20\%B_0)$	0.173	0.170	0.180	0.176
$\Pr(< 10\%B_0)$	0.000	0.000	0.000	0.000
$\%B_0^r$	0.098 (0.073–0.130)	0.10 (0.069–0.141)	0.102 (0.065–0.150)	0.105 (0.062–0.159)
$\%B_{ref}^r$	0.412 (0.300–0.566)	0.420 (0.286–0.601)	0.428 (0.270–0.638)	0.439 (0.263–0.676)
$\Pr(> B_{ref}^r)$	0.000	0.000	0.000	0.000
$\Pr(> B_{msy}^r)$	0.006	0.026	0.054	0.089
$\Pr(> B_{current}^r)$		0.624	0.644	0.679

Table 12: Summary of key indicators from the projection for the base case MCMC with future commercial catch set to 90% of current TACC: projected biomass as a percentage of the virgin and current stock status, for spawning stock and recruit-sized biomass, respectively.

90% TACC	2011	2012	2013	2014
$\%B_0$	0.221 (0.180–0.272)	0.227 (0.177–0.287)	0.236 (0.177–0.307)	0.244 (0.175–0.326)
$\%B_{ref}$	0.655 (0.537–0.805)	0.673 (0.535–0.847)	0.700 (0.532–0.913)	0.724 (0.525–0.974)
$\Pr(> B_{ref})$		0.000	0.002	0.015
$\Pr(> B_{current})$	*0.000*	*0.662*	*0.749*	*0.796*
$\Pr(< 20\%B_0)$	0.173	0.150	0.126	0.112
$\Pr(< 10\%B_0)$	0.000	0.000	0.000	0.000
$\%B_0^r$	0.098 (0.073–0.130)	0.102 (0.071–0.143)	0.109 (0.072–0.157)	0.117 (0.074–0.171)
$\%B_{ref}^r$	0.412 (0.300–0.566)	0.430 (0.295–0.612)	0.458 (0.299–0.673)	0.490 (0.309–0.732)
$\Pr(> B_{ref}^r)$		0.000	0.000	0.000
$\Pr(> B_{current}^r)$	0.000	0.763	0.871	0.926

Table 13: Summary of key indicators from the projection for the base case MCMC with future commercial catch set to 85% of current TACC: projected biomass as a percentage of the virgin and current stock status, for spawning stock and recruit-sized biomass, respectively.

Projection under 85% TACC	2011	2012	2013	2014
$\%B_0$	0.221 (0.180–0.272)	0.228 (0.179–0.288)	0.239 (0.180–0.310)	0.250 (0.180–0.331)
$\%B_{ref}$	0.655 (0.537–0.805)	0.677 (0.538–0.850)	0.710 (0.541–0.923)	0.740 (0.541–0.990)
$\Pr(> B_{ref})$	0	0.000	0.003	0.021
$\Pr(> B_{current})$		0.701	0.803	0.854
$\Pr(< 20\%B_0)$	0.1726	0.139	0.108	0.086
$\Pr(< 10\%B_0)$	0	0	0	0
$\%B_0^r$	0.098 (0.073–0.130)	0.103 (0.072–0.144)	0.113 (0.076–0.161)	0.123 (0.080–0.177)
$\%B_{ref}^r$	0.412 (0.300–0.566)	0.435 (0.299–0.618)	0.474 (0.312–0.691)	0516 (0.333–0.761)
$\Pr(> B_{ref}^r)$	0	0.000	0.000	0.000
$\Pr(> B_{current}^r)$		0.829	0.940	0.975

Table 14: Summary of key indicators from the projection for the base case MCMC with future commercial catch set to 80% of current TACC: projected biomass as a percentage of the virgin and current stock status, for spawning stock and recruit-sized biomass, respectively.

Projection under 80% TACC	2011	2012	2013	2014
$\%B_0$	0.221 (0.180–0.272)	0.229 (0.180–0.289)	0.242 (0.184–0.313)	0.255 (0.185–0.336)
$\%B_{ref}$	0.655 (0.537–0.805)	0.680 (0.541–0.853)	0.719 (0.550–0.933)	0.756 (0.557–1.006)
$\Pr(> B_{ref})$	0.000	0.000	0.005	0.029
$\Pr(> B_{current})$		0.740	0.851	0.897
$\Pr(< 20\%B_0)$	0.173	0.126	0.089	0.063
$\Pr(< 10\%B_0)$	0.000	0.000	0.000	0.000
$\%B_0^r$	0.098 (0.073–0.130)	0.104 (0.073–0.145)	0.117 (0.080–0.165)	0.129 (0.086–0.184)
$\%B_{ref}^r$	0.412 (0.300–0.566)	0.440 (0.303–0.623)	0.489 (0.327–0.709)	0.542 (0.356–0.790)
$\Pr(> B_{ref}^r)$	0.000	0.000	0.000	0.000
$\Pr(> B_{current}^r)$		0.884	0.977	0.995

Table 15: Inputs for projections under various scenarios of area-alienation. Mean sub-area catch is from 2006–2011.

Scenario	Closed sub-areas	In assessment area ?	Mean sub-area catch (kg)	Projected catch in model (kg)	Proportion Alienation
1				199 716	
2	Tory	Y	6 990	199 716	0.035
3	D'Urville	Y	17 377	199 716	0.120
3A	D'Urville	Y	17 377	180 992	0.120
3B				171 630	0.120
3C				162 268	0.120
4	West coast	N	6 175	205 891	0.120
4A				187 167	0.120
4B				177 805	0.120
4C				168 443	0.120

Table 16: Projected spawning biomass and indicators under various area-alienation scenarios (see Table 15).

Scenario	B_{2011}	B_{2012}	B_{2013}	B_{2014}	$\Pr(B_{2012} < B_{2011})$	$\Pr(B_{2013} < B_{2011})$	$\Pr(B_{2014} < B_{2011})$
1	933	948	969	987	0.408	0.363	0.329
2	933	911	925	935	0.681	0.553	0.503
3	933	822	818	807	0.985	0.922	0.882
3a	933	832	845	852	0.976	0.862	0.778
3b	933	836	859	874	0.968	0.824	0.717
3c	933	841	872	896	0.962	0.782	0.643
4	933	819	809	792	0.988	0.936	0.905
4a	933	829	836	837	0.980	0.882	0.816
4b	933	833	850	859	0.973	0.852	0.758
4c	933	838	863	882	0.966	0.811	0.691

Table 17: Projected recruit-sized biomass and indicators under various area-alienation scenarios (see Table 15).

Scenario	B^r_{2011}	B^r_{2012}	B^r_{2013}	B^r_{2014}	$\Pr(B^r_{2012} < B^r_{2011})$	$\Pr(B^r_{2013} < B^r_{2011})$	$\Pr(B^r_{2014} < B^r_{2011})$
1	334	340	347	357	0.376	0.356	0.321
2	334	325	326	329	0.662	0.597	0.536
3	334	289	274	261	0.995	0.970	0.949
3a	334	297	299	302	0.982	0.879	0.773
3b	334	301	311	323	0.974	0.775	0.600
3c	334	305	323	344	0.955	0.633	0.411
4	334	286	265	248	0.997	0.984	0.973
4a	334	294	290	289	0.989	0.923	0.855
4b	334	298	303	309	0.980	0.848	0.723
4c	334	302	315	330	0.967	0.732	0.533

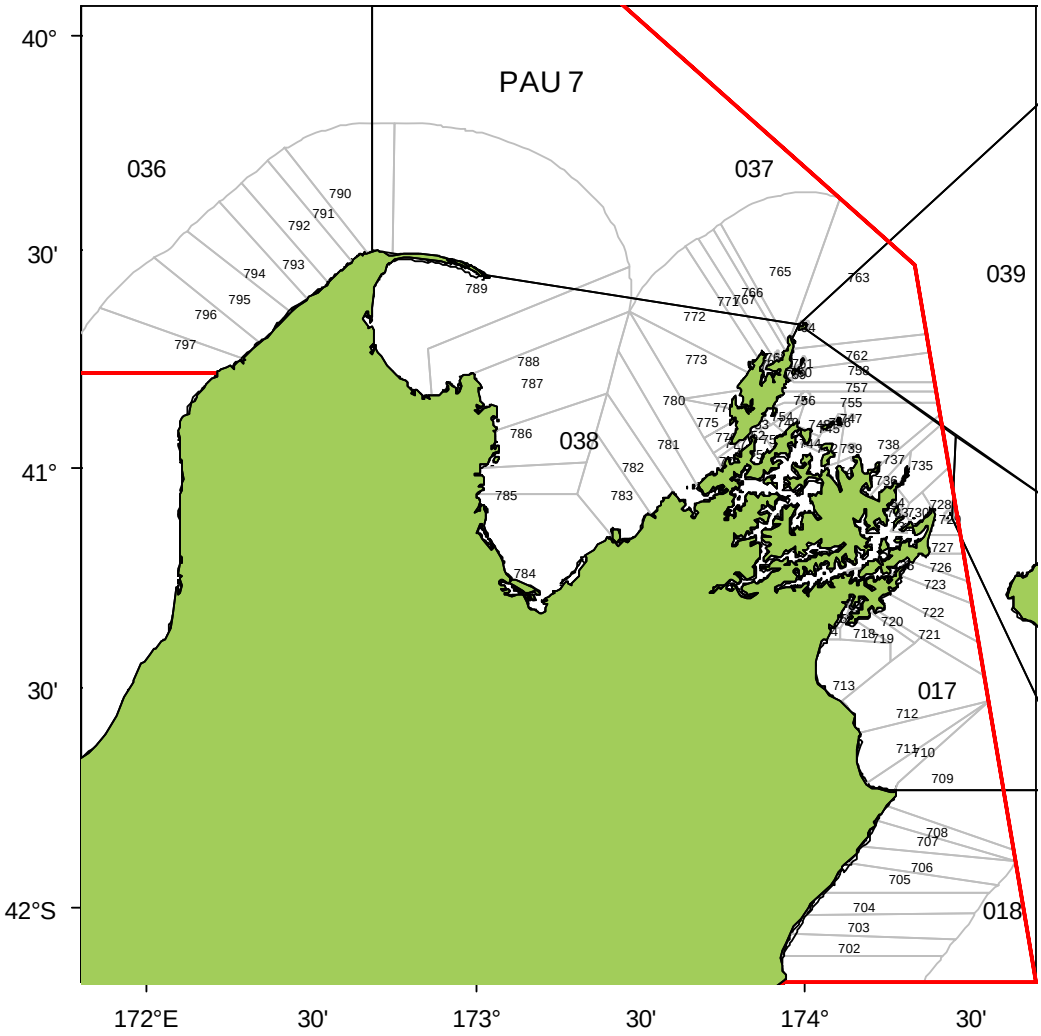

Figure 1: Map of PAU 7 showing the boundaries of the general statistical areas and the new finer scale Paua statistical areas.

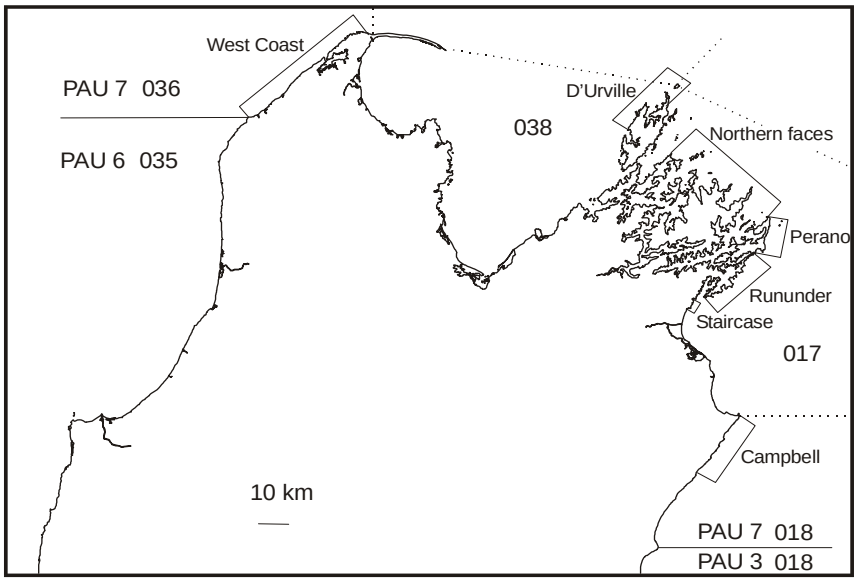

Figure 2: Research survey strata within PAU 7.

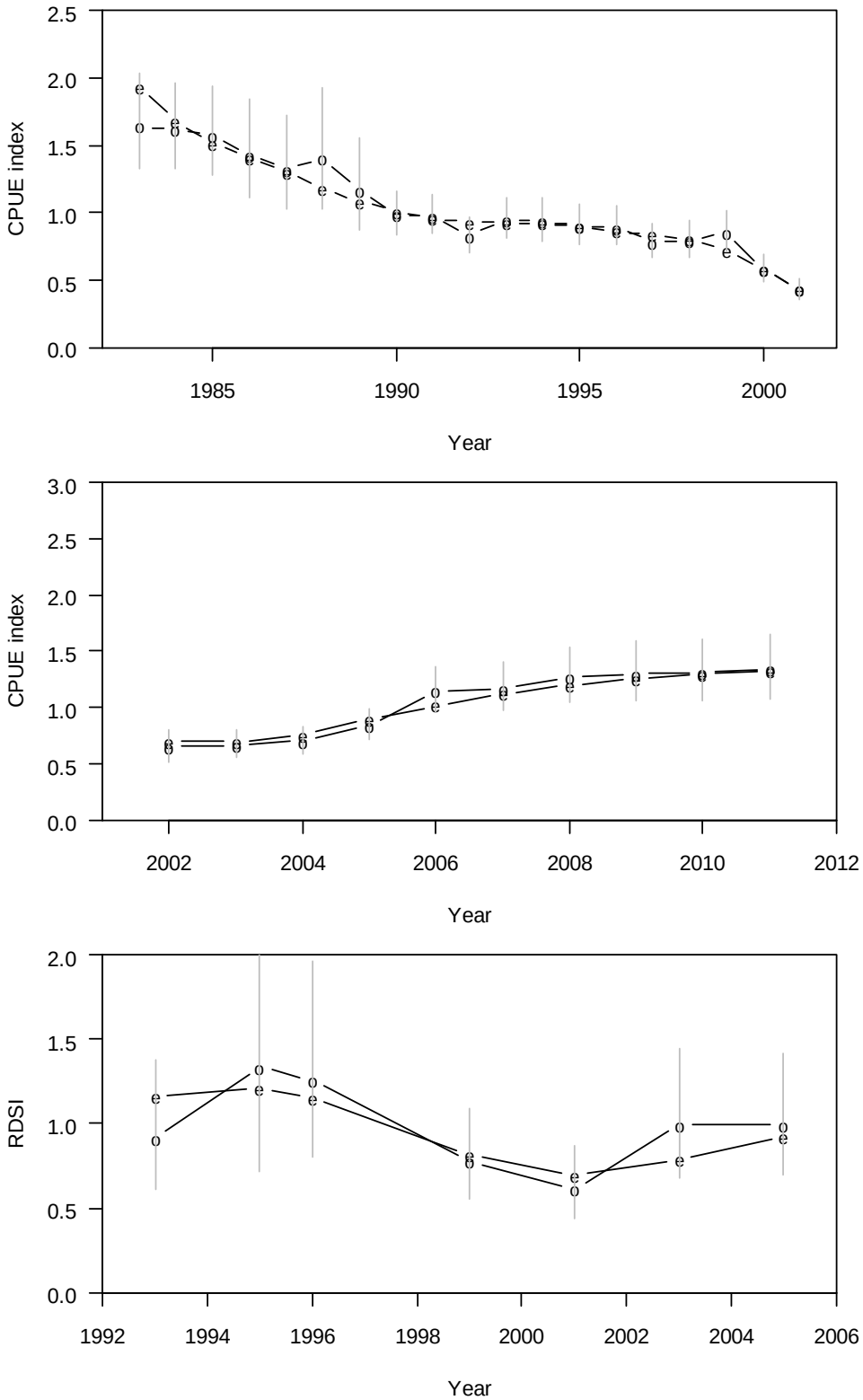

Figure 3: MPD fits to the CPUE indices (top), PCPUE indices (middle), and RDSI (bottom) for the base case model (1.0).

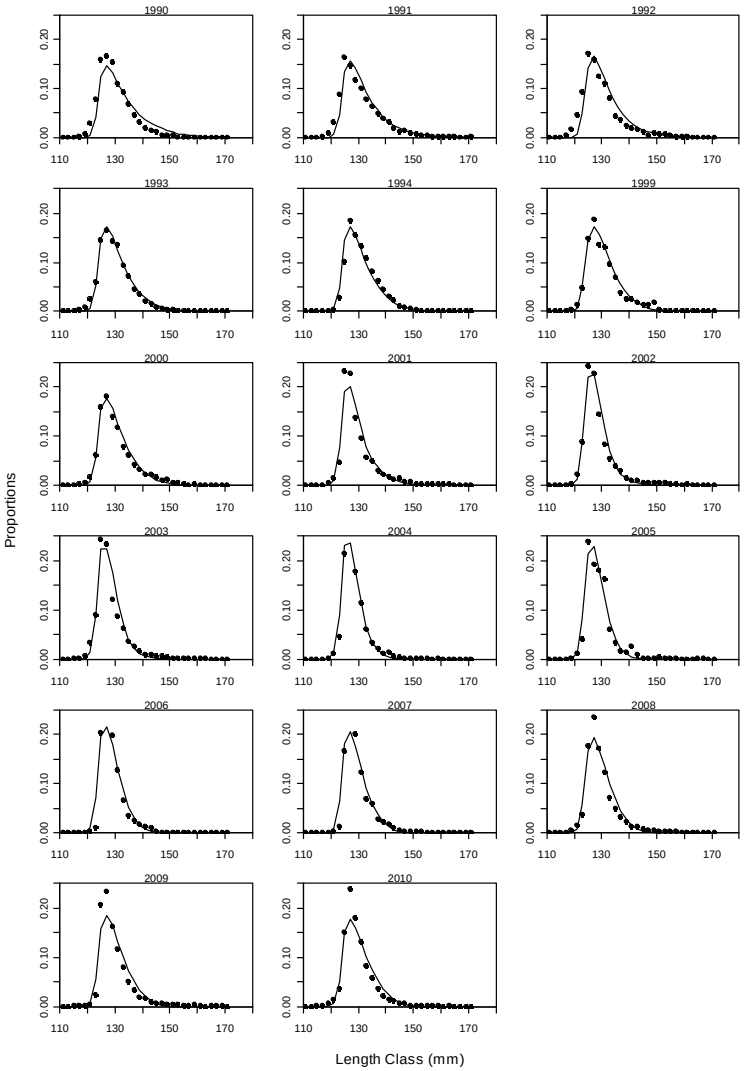

Figure 4: MPD fits to the CSLF data for the base case model (1.0).

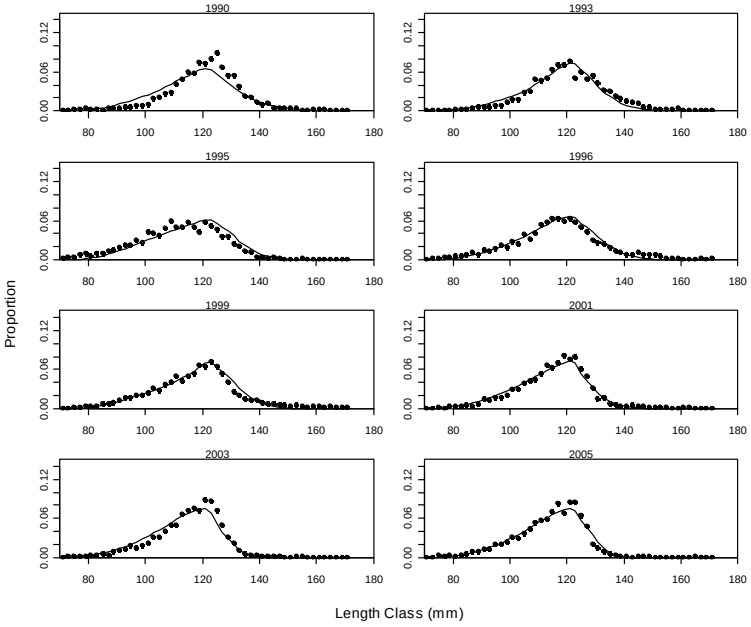

Figure 5: MPD fits to the RDLF data for the base case model (1.0).

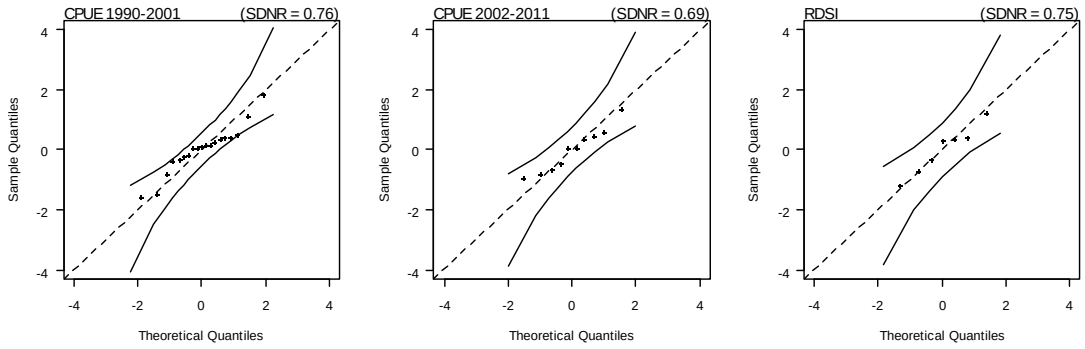

Figure 6: Normal Q-Q plots for residuals from fits to the three abundance datasets for the MPD base case model (1.0).

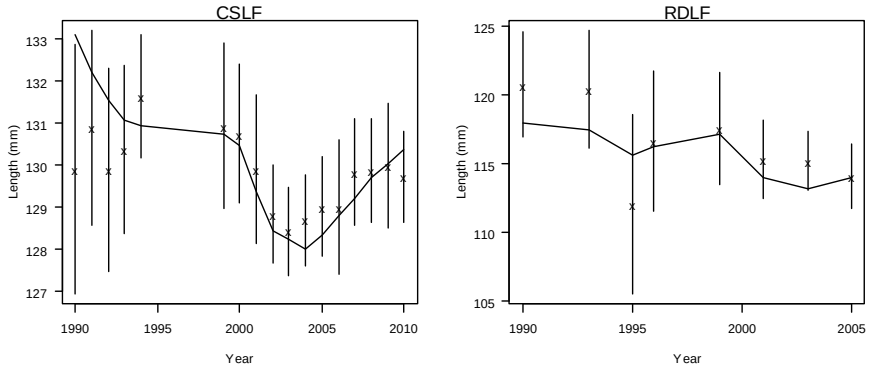

Figure 7: Observed and predicted mean length by year for the CSLF and RDLF datasets for MPD base case model (1.0). The vertical lines are confidence interval for the mean length.

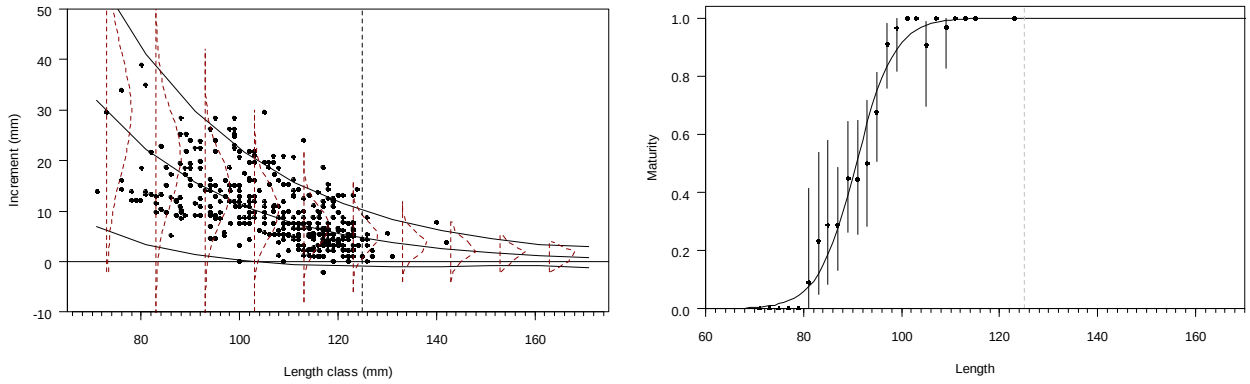

Figure 8: MPD fits to the tag-recapture data (left: The dots are observed mean annual increments; the black lines are the fitted growth curve with 95% confidence intervals; dashed lines are from the estimated growth transition matrix at selected sizes) and maturity data (right: dots are observed proportion mature at length with confidence interval; the lines are predicted proportion of maturity at length) for base case model (1.0).

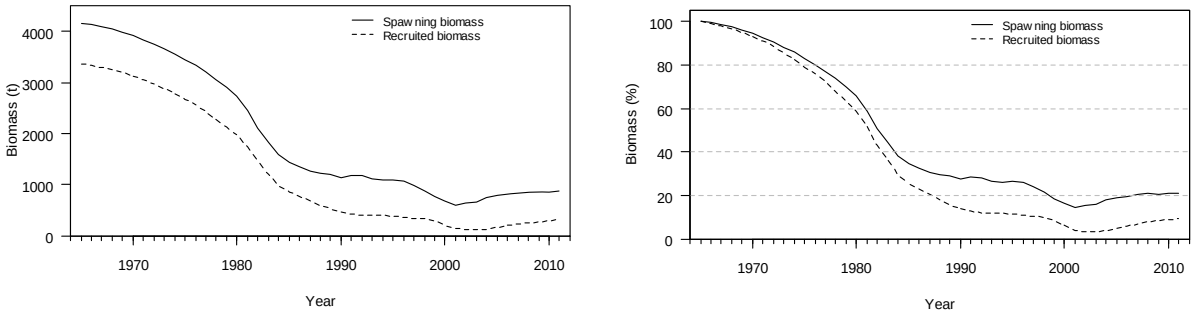

Figure 9: Estimated spawning and recruit-sized biomass (left) and spawning and recruit-sized biomass as a percentage of the virgin level (right) for MPD base case model (1.0).

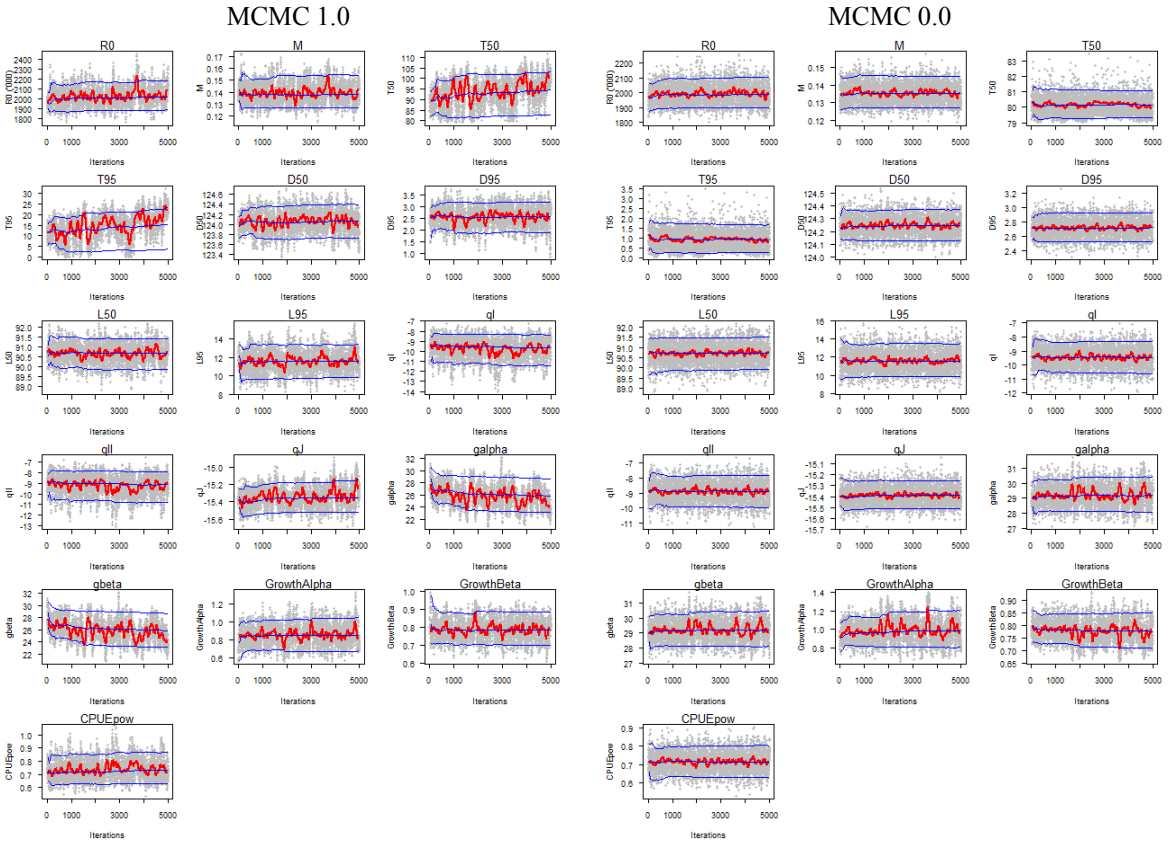

Figure 10: Traces of estimated parameters for base case MCMC 1.0 (left), and initial model MCMC 0.0 (right).

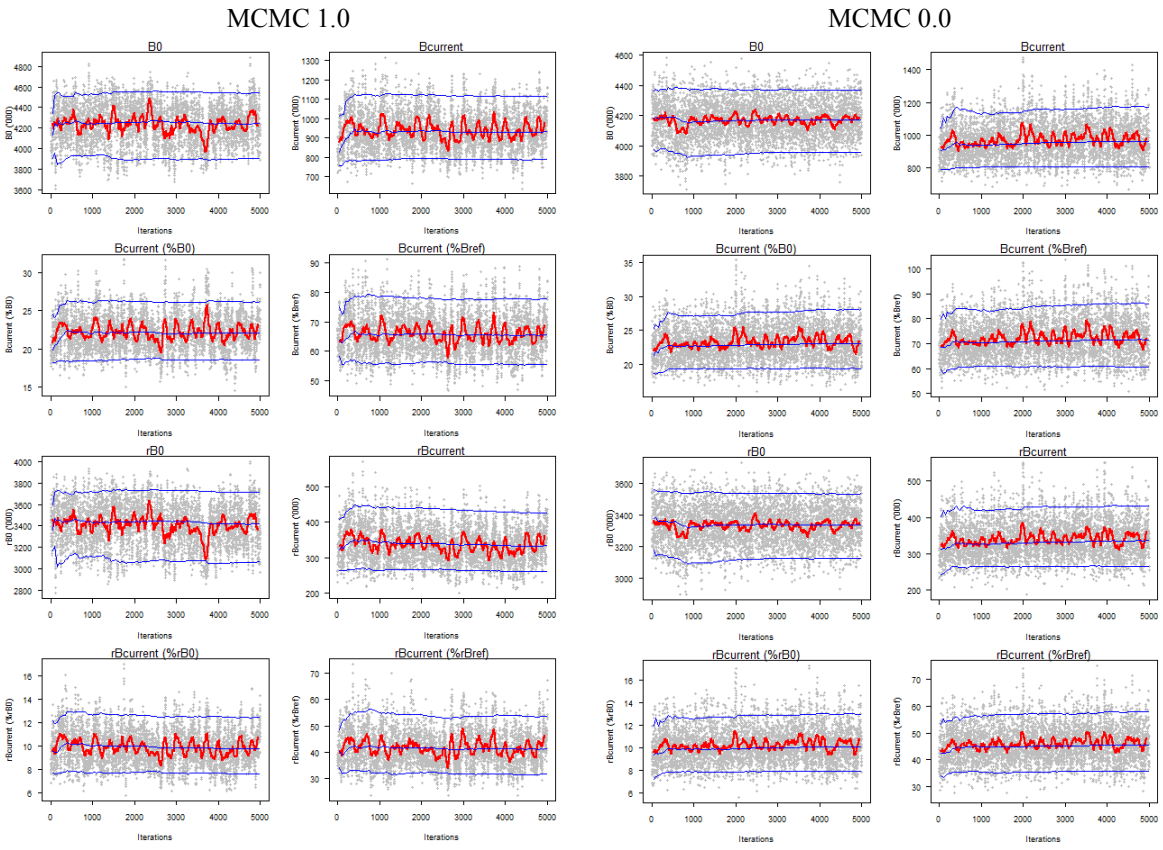

Figure 11: Traces of biomass indicators for base case MCMC 1.0 (left), and initial model MCMC 0.0 (right).

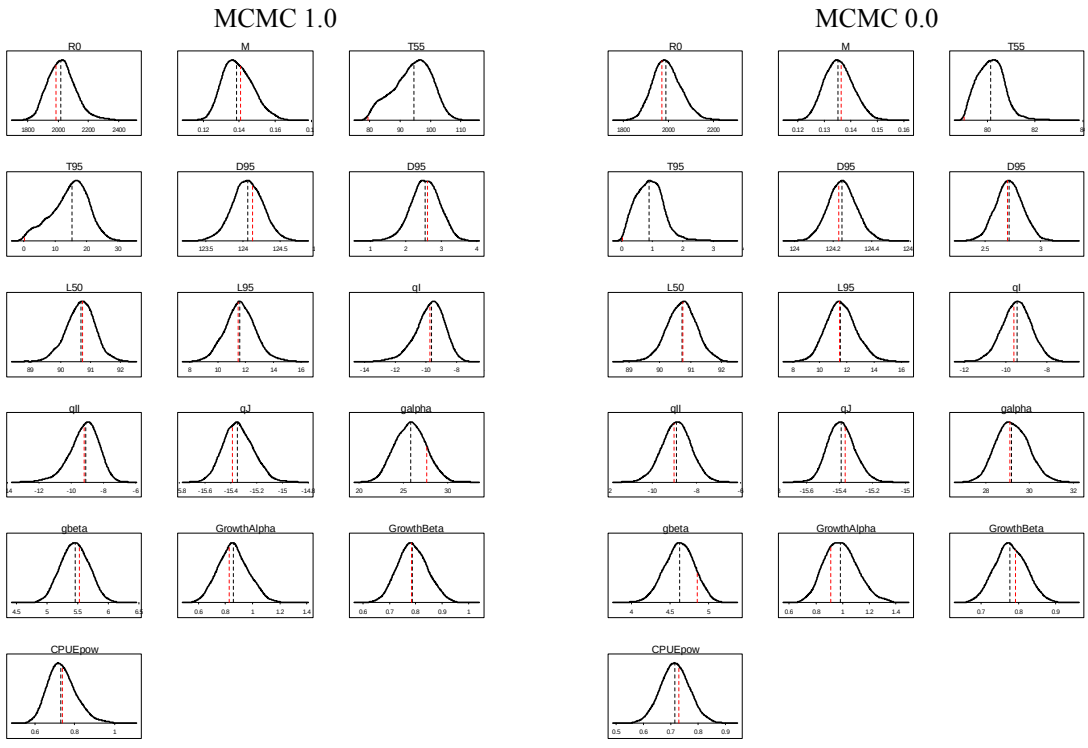

Figure 12: Posterior distributions of estimated parameters for base case MCMC 1.0 (left), and initial model MCMC 0.0 (right). The black dashed lines are the posterior median and red line and the red dashed lines are the MPD estimates.

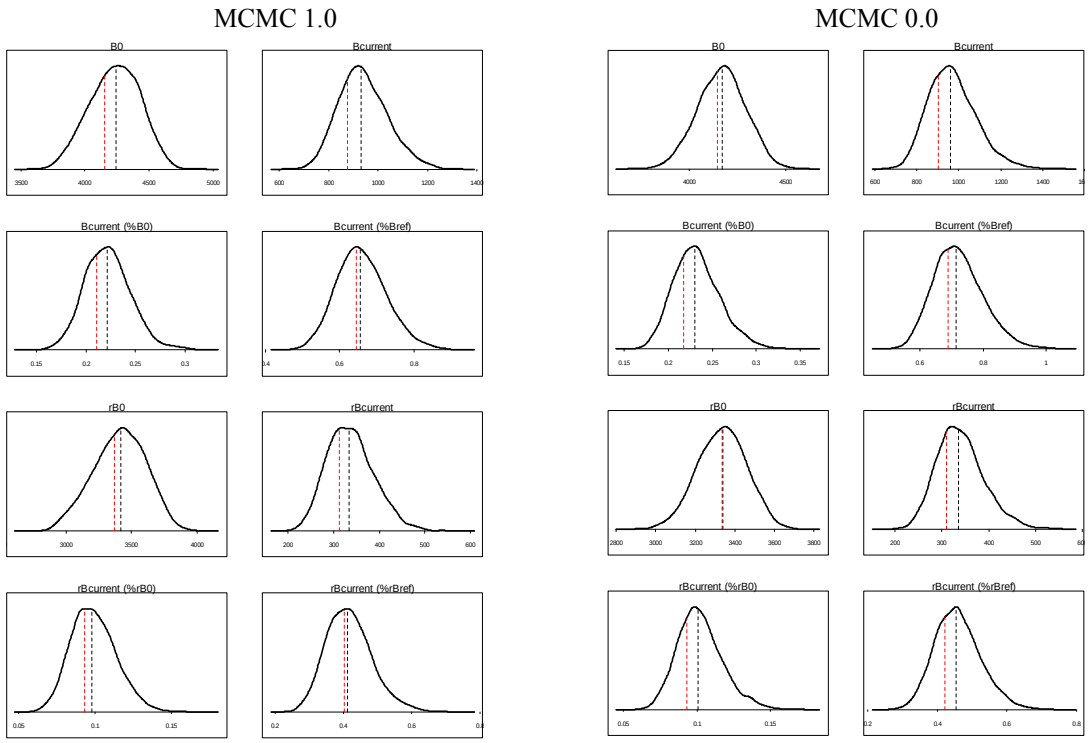

Figure 13: Posterior distributions of biomass indicators for base case MCMC 1.0 (left), and initial model MCMC 0.0 (right). The black dashed lines are the posterior median and red line and the red dashed lines are the MPD estimates.

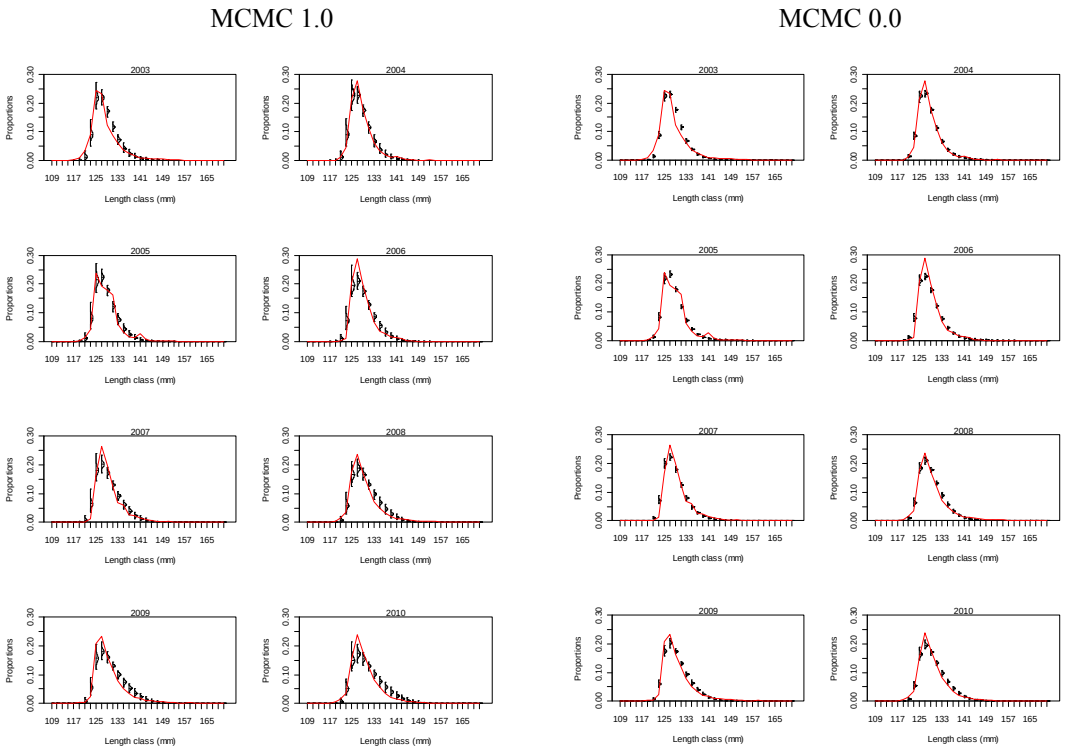

Figure 14: Posterior of the fits to the CSLF for selected years from MCMC 1.0 (left) and MCMC 0.0 (right).

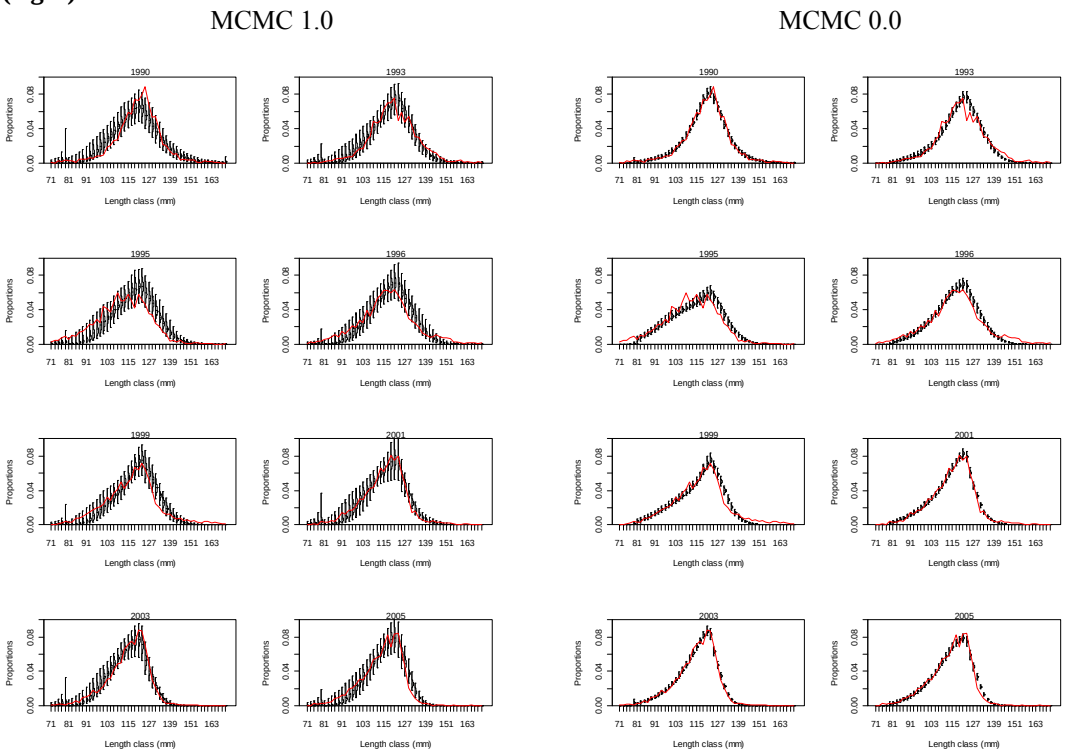

Figure 15: Posterior of the fits to the RDLF from MCMC 1.0 (left) and MCMC 0.0 (right).

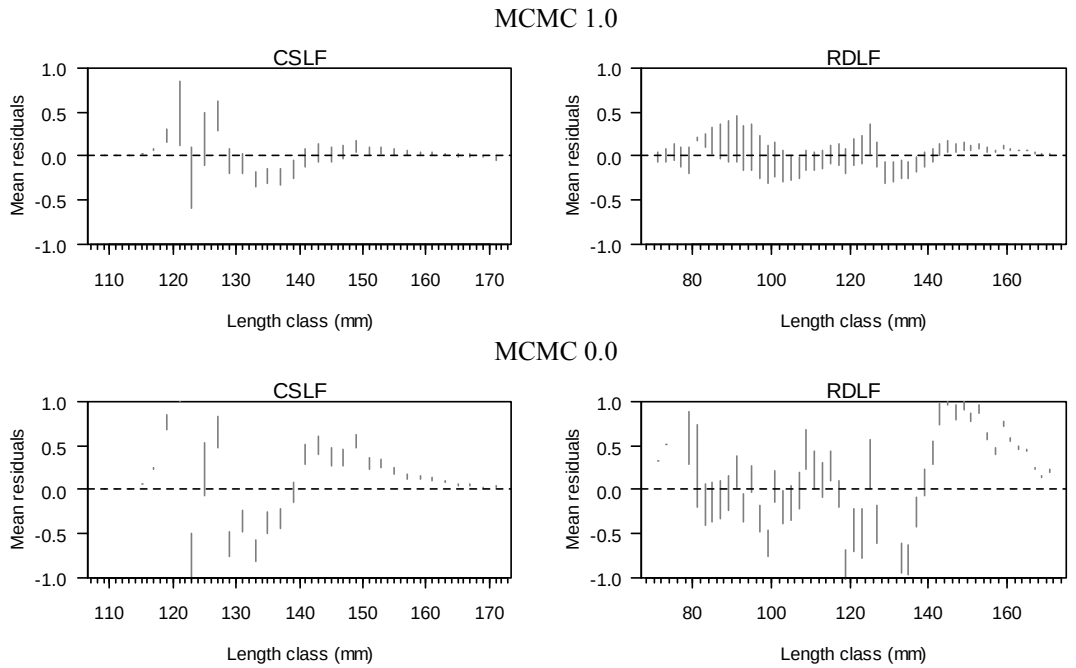

Figure 16: 95% credible intervals of the posterior distributions of mean residuals (across all years) of fits to the CSLF and RDLF data from MCMC 1.0 (top) and MCMC 0.0 (bottom).

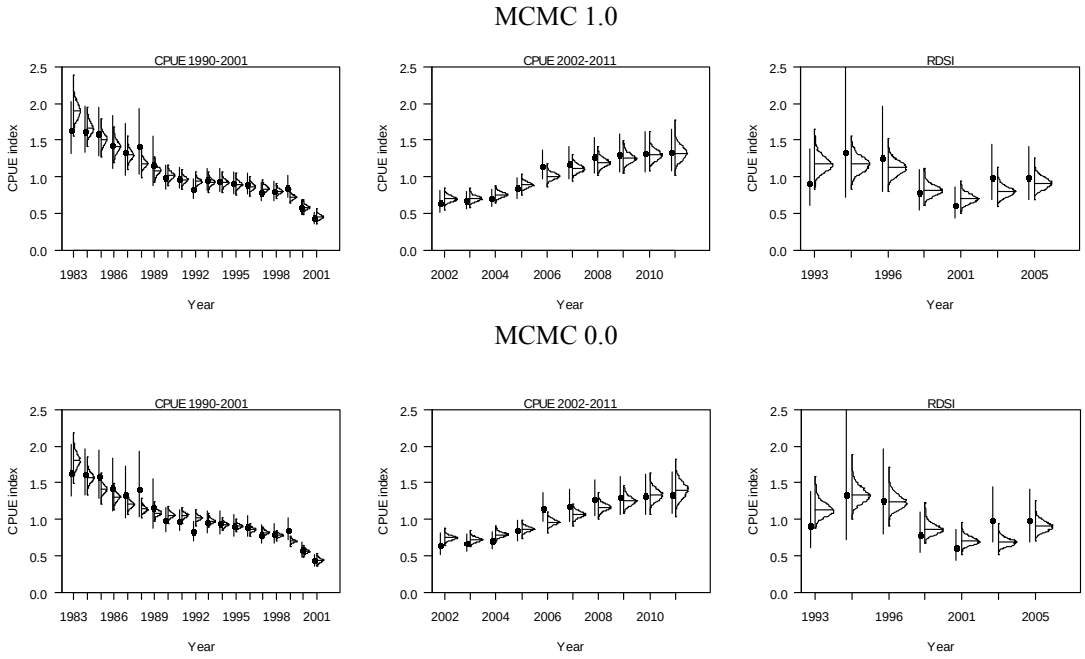

Figure 17: Posterior of the fits to the abundance data from MCMC 1.0 and MCMC 0.0.

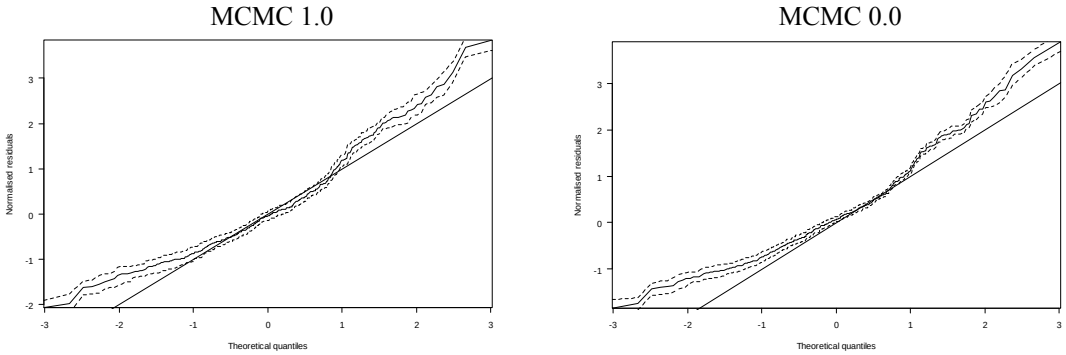

Figure 18: Q-Q plots of the residuals (median and 95% credible interval) of the fits to the tag-recapture data from MCMC 1.0 (left) and MCMC 0.0 (right).

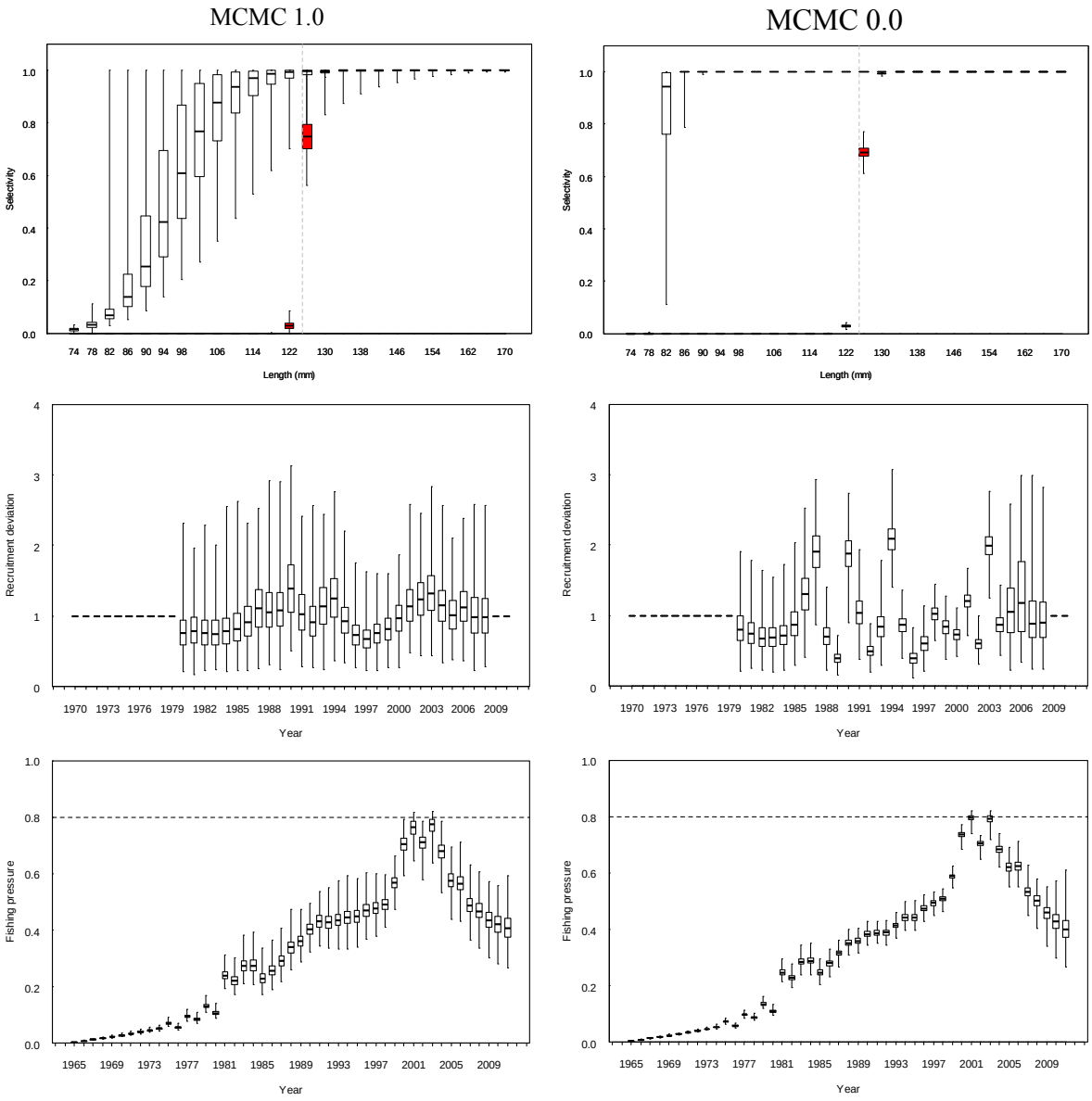

Figure 19: Posterior distributions of estimated commercial and research diver selectivity (top), recruitment deviations (middle), and exploitation rates (bottom) for the MCMC 1.0 (left) and MCMC 0.0 (right). The box shows the median of the posterior distribution (horizontal bar), the 25th and 75th percentiles (box), with the whiskers representing the full range of the distribution. Recruitment deviations were estimated for 1980–2008, and fixed at 1 for other years.

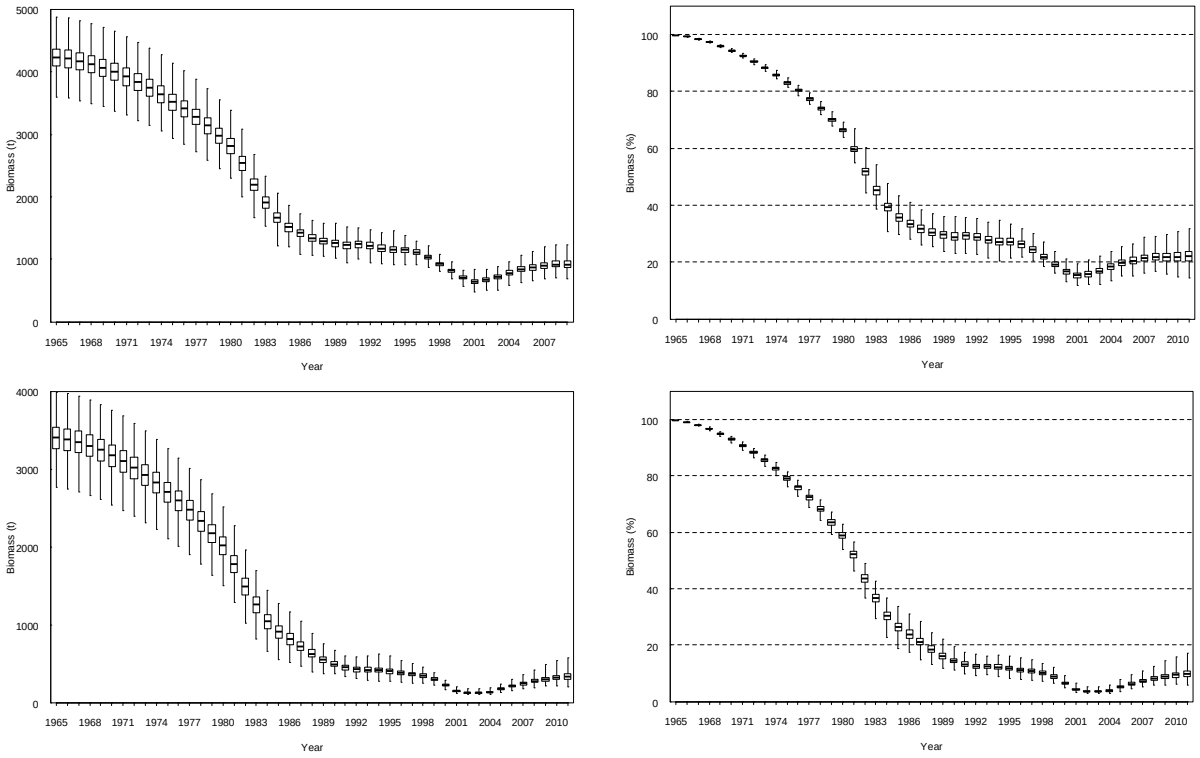

Figure 20: Posterior distributions of spawning stock biomass and spawning stock biomass as a percentage of virgin level (top panel), recruit-sized biomass and recruit-sized biomass as a percentage of virgin level (bottom panel) from MCMC 1.0. The box shows the median of the posterior distribution (horizontal bar), the 25th and 75th percentiles (box), with the whiskers representing the full range of the distribution.

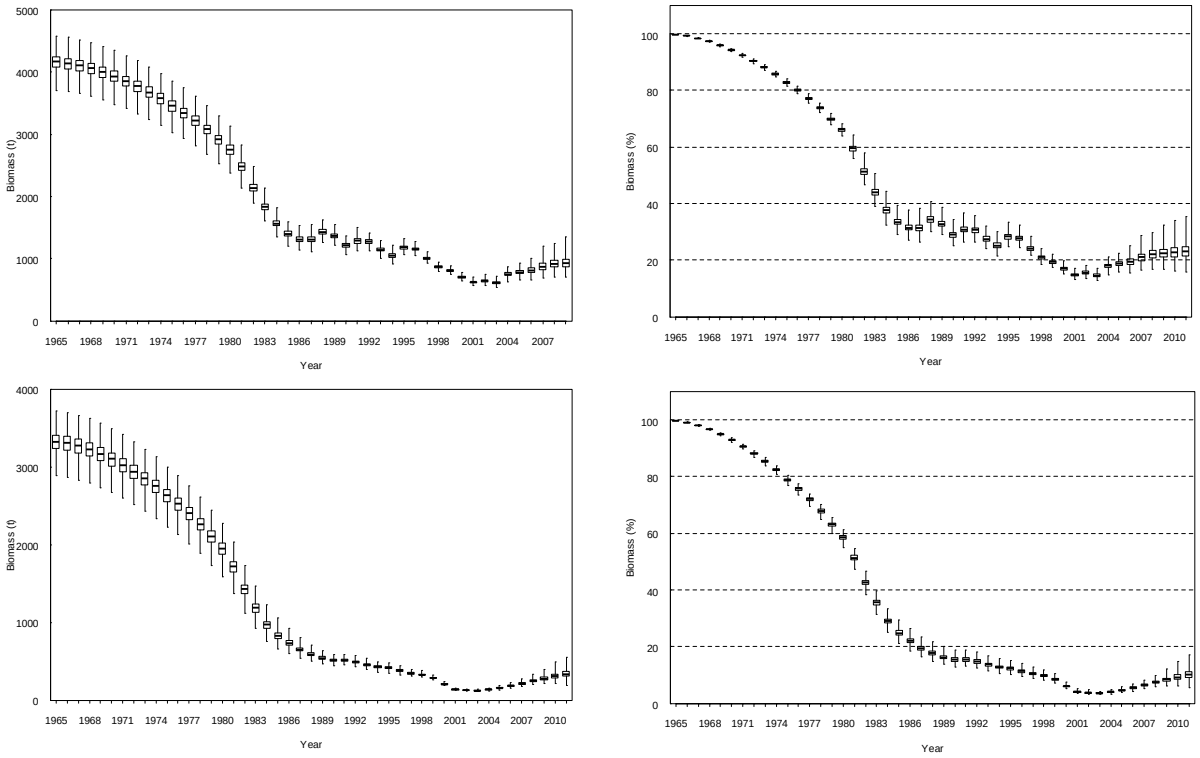

Figure 21: Posterior distributions of spawning stock biomass and spawning stock biomass as a percentage of virgin level (top panel), recruit-sized biomass and recruit-sized biomass as a percentage of virgin level (bottom panel) from MCMC 0.0. The box shows the median of the posterior distribution (horizontal bar), the 25th and 75th percentiles (box), with the whiskers representing the full range of the distribution.

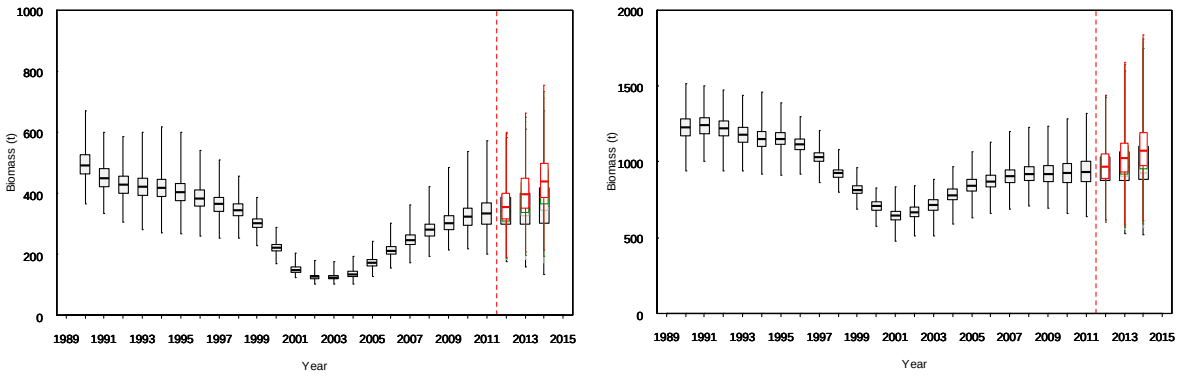

Figure 22: Posterior distributions of projected spawning stock and recruit-sized biomass under four scenarios of assumed future catch levels (100%, 90%, 85%, and 80% of TACC) for MCMC 1.0 (base case). The box shows the median of the posterior distribution (horizontal bar), the 25th and 75th percentiles (box), with the whiskers representing the full range of the distribution.

APPENDIX A: SUMMARY MPD MODEL FITS AND ESTIMATES

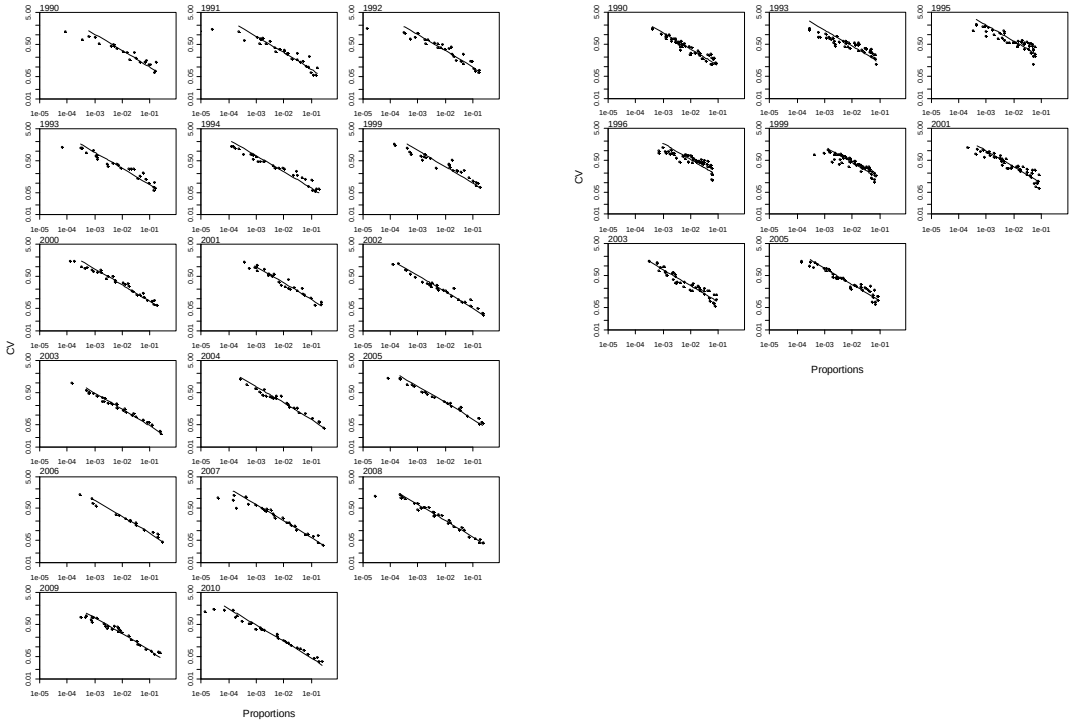

Figure A1: Estimated proportions versus c.v.s for the commercial catch length frequencies for 1990–1994 and 1999–2009 (left) and for the research diver length frequencies for 1990, 1993, 1995, 1996, 1999, 2001, 2003, and 2005 (right) in PAU 7 . Lines indicate the best least squares fit for the effective sample size of the multinomial distribution.

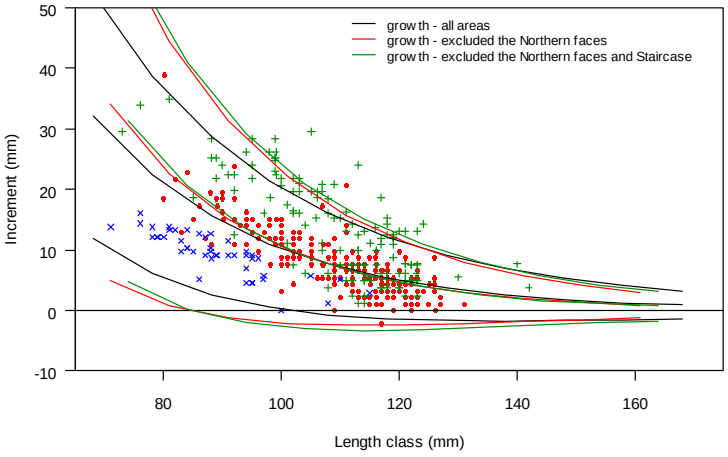

Figure A2: Estimated growth curves when different subsets of tag-recapture data were included (based on the initial model): with all the growth data, with growth data from the Northern faces being excluded, and with growth data from the Northern faces and Staircase being excluded.

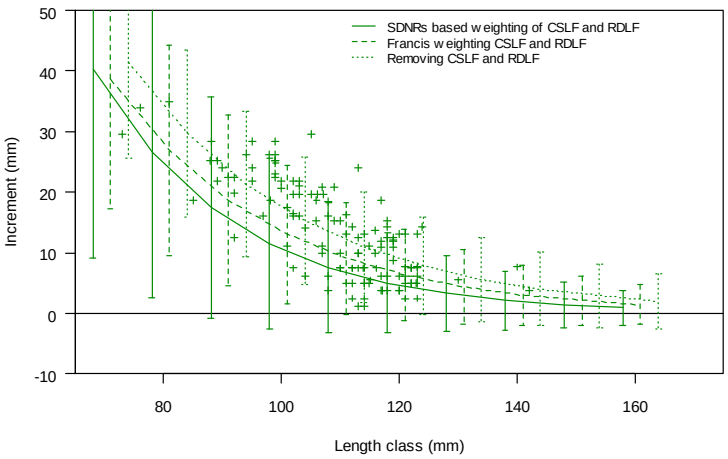

Figure A3: Estimated growth curves when growth data from Northern faces and Staircase were excluded from three model runs: weighting of CSLF and RDLF were based on balanced SDNRs; CSLF and RDLF were down-weighted using Francis method; CSLF and RDLF were removed.

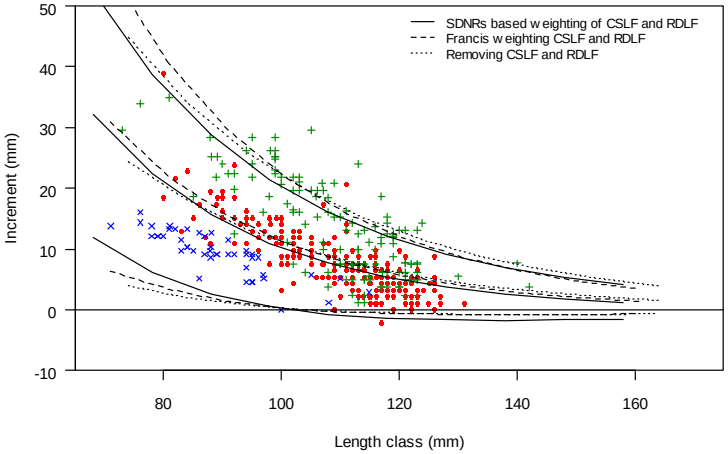

Figure A4: Estimated growth curves when growth data from all the areas were included from three model runs: weighting of CSLF and RDLF were based on balanced SDNRs; CSLF and RDLF were down-weighted using Francis method; CSLF and RDLF were removed.

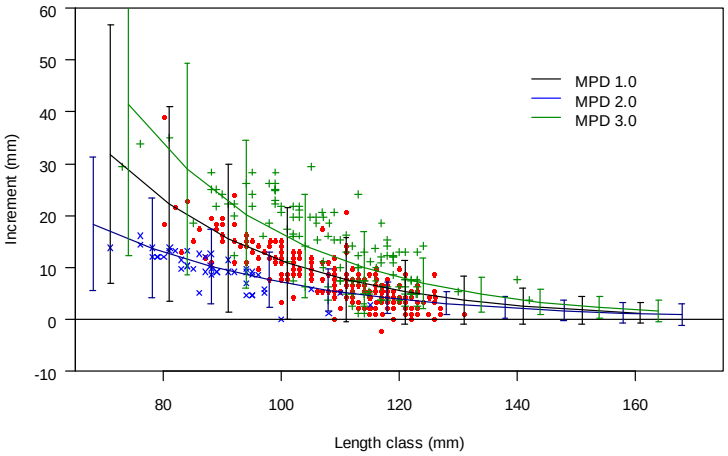

Figure A5: Growth curves used in various model runs. For base case, growth parameters were estimated in the model by fitting to annual growth increments data from Rununder and Perano (green), Northern faces (red), and Staircase (blue). For model 2.0, growth parameters were fixed with $g_1 = 15$, $g_2 = 5$, and $\varphi = 0.35$. For model 3.0, growth parameters were fixed with $g_1 = 40$, $g_2 = 8$, and $\varphi = 0.35$.

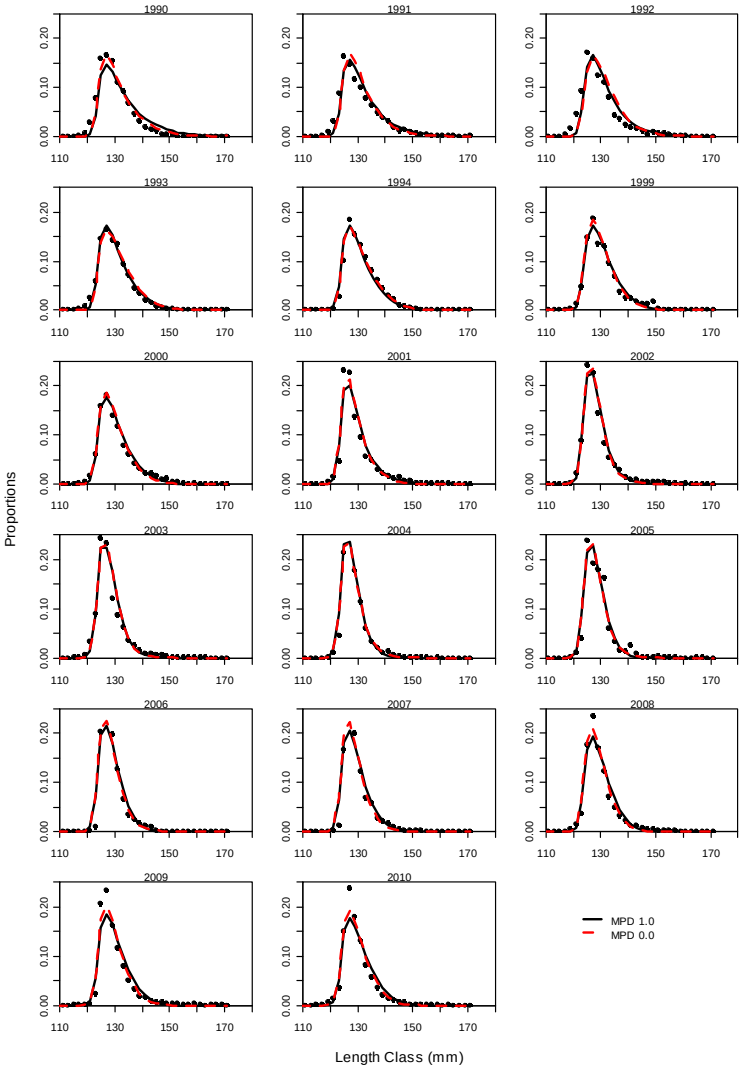

Figure A6: Comparison of fits to the CSLF data for between MPD 1.0 (base case) and initial model (0.0).

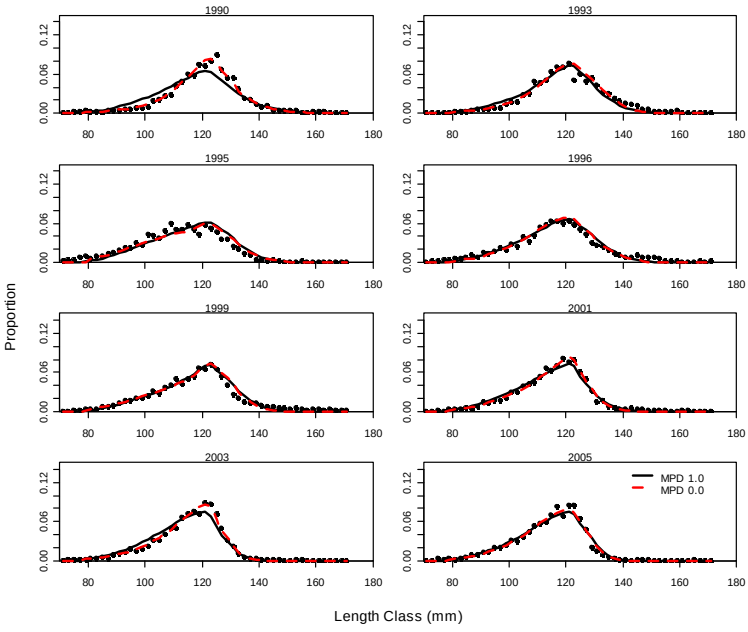

Figure A7: Comparison of fits to the RDLF data for between MPD 1.0 (base case) and initial model (0.0).

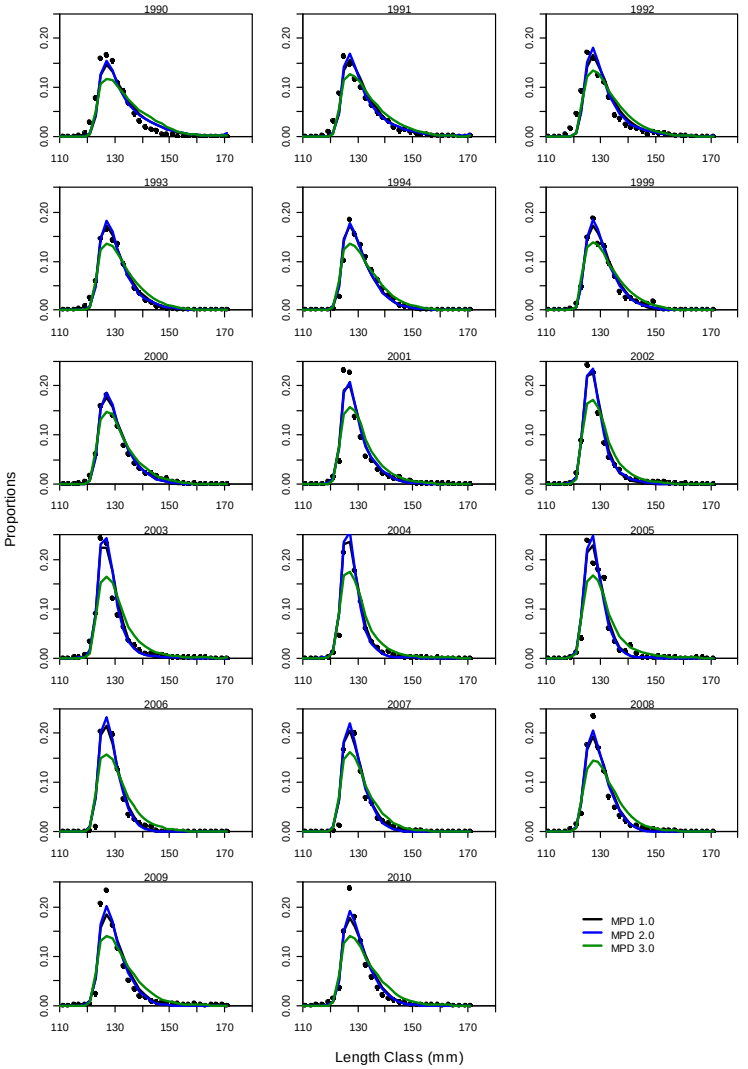

Figure A8: Comparison of fits to the CSLF data between MPD models 1.0, 2.0, and 3.0.

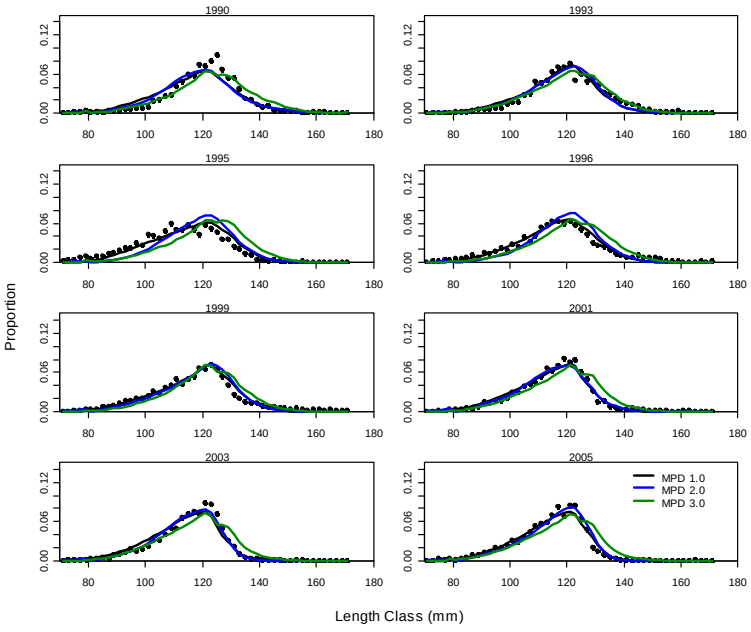

Figure A9: Comparison of fits to the RDLF data for between MPD models 1.0, 2.0, and 3.0.

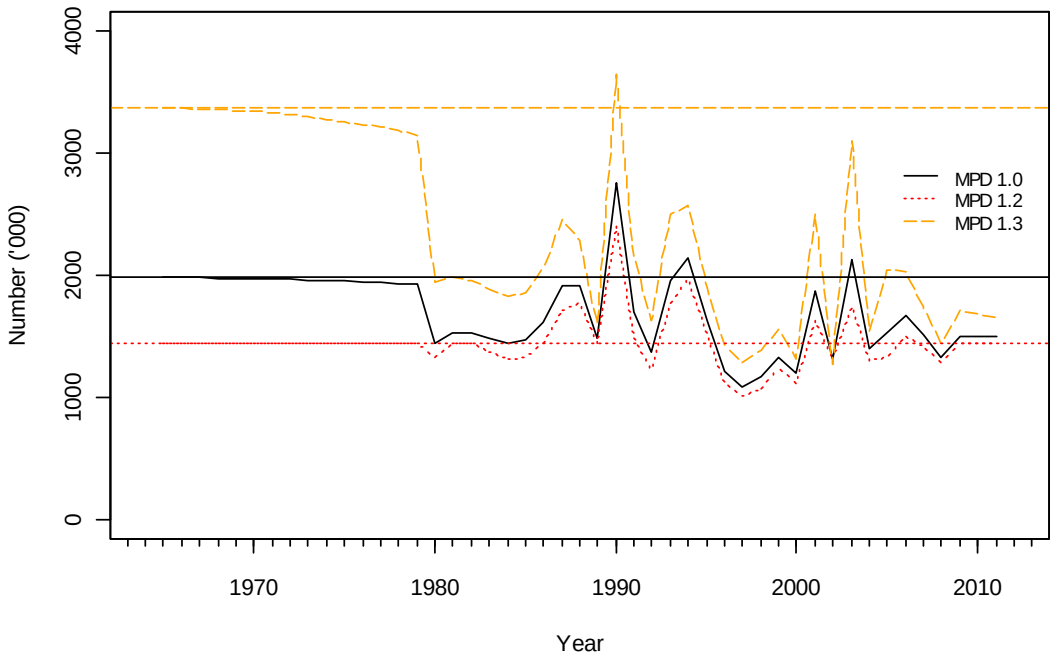

Figure A10: Comparison of estimated annual recruits between MPD models 1.0, 1.2, and 1.3.

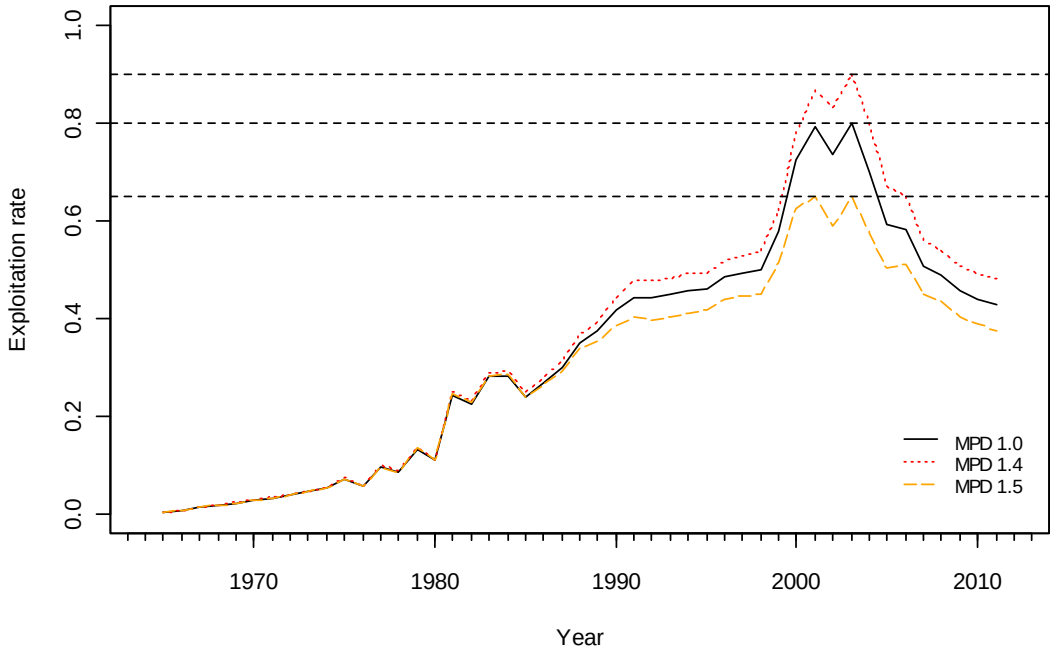

Figure A11: Comparison of estimated exploitation rates between MPD models 1.0, 1.4, and 1.5.

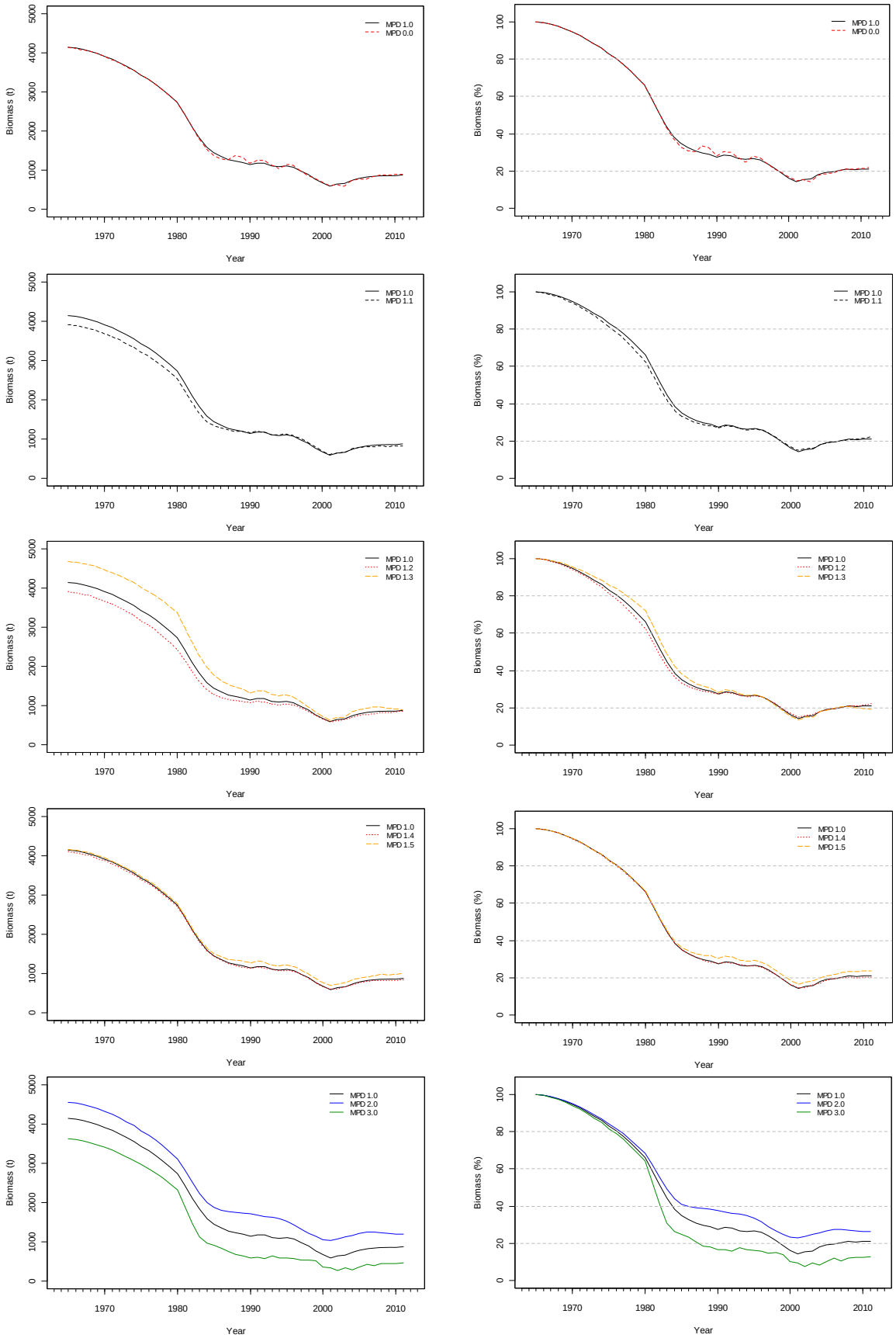

Figure A12: Comparison of estimated spawning stock biomass (left) and spawning stock biomass as a percentage of virgin level (right) between MPD base case and sensitivity runs.